Germany
(June 2011)

Large-Scale Ab Initio Simulations for Biomolecular Systems

Shigenori Tanaka

Graduate School of System Informatics

Kobe University

Contents

- Ab initio simulations for biomolecular systems
  - Descriptions of electronic states
    - Influenza viral proteins
  - Descriptions of charge and energy transfer dynamics
    - Photosynthetic systems

Fragment Molecular Orbital (FMO) method

Problems of existing approaches to biomolecules:

- Classical force field is **empirical** for inter-molecular interactions.
- Conventional quantum mechanical calculations is too **expensive**.

Our approach: The FMO method

- FMO method was proposed by Kitaura *et al.* (1999).
- Molecules are divided into **fragments.**

- Whole molecular energies are calculated by the sum of fragment and fragment-pair energies.

  → Drastic speed up has been attained !

- Error of FMO total energy is within 0.4 kcal/mol for crambin (46 residues).

Advantage of FMO method: Molecular interaction analysis

- Molecular interaction analysis : receptor-ligand binding
- Inter-fragment interaction energy (IFIE) analysis

FMO Method and Its Energy Analysis (IFIE)

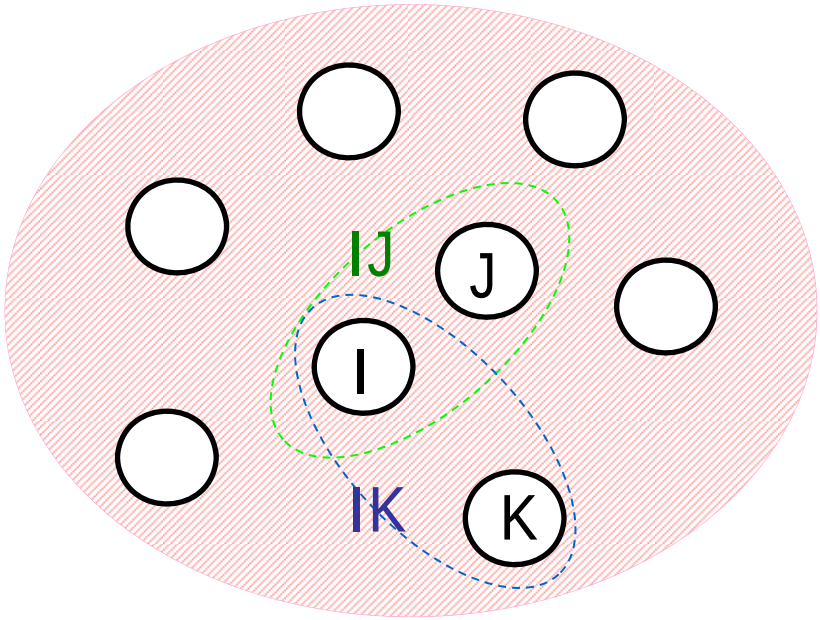

Divide a molecule into fragments

- N pieces of fragments
- [N(N-1)/2] pieces of fragment pairs

Total Energy : Calculated from energies of fragments and fragment pairs

$$E = \sum_{I>J} E_{IJ} - (N-2)\sum_{I} E_I$$

Inter-Fragment Interaction Energy (IFIE) :

$$\Delta E_{IJ} = (E'_{IJ} - E'_I - E'_J) + \mathrm{Tr}(\Delta P_{IJ} V_{IJ})$$

E_X : energies of a fragment and a fragment pair

V_X : Electrostatic potential from surrounding fragments

$$E'_X = E_X - V_X$$

Fragment Molecular Orbital Method

$$H_I = \sum_{i\in I}\left\{\left(-\frac{1}{2}\nabla_i^2\right)+\sum_A\left(-\frac{Z_A}{|\mathbf{r}_i-\mathbf{A}|}\right)+\sum_{J\neq I}^{N}\int\frac{\rho_J(\mathbf{r}')}{|\mathbf{r}_i-\mathbf{r}'|}d\mathbf{r}'\right\}+\sum_{i\in I}\sum_{i>j\in I}\frac{1}{|\mathbf{r}_i-\mathbf{r}_j|}$$

$$H_{IJ} = \sum_{i\in I,J}\left\{\left(-\frac{1}{2}\nabla_i^2\right)+\sum_A\left(-\frac{Z_A}{|\mathbf{r}_i-\mathbf{A}|}\right)+\sum_{K\neq I,J}^{N}\int\frac{\rho_K(\mathbf{r}')}{|\mathbf{r}_i-\mathbf{r}'|}d\mathbf{r}'\right\}+\sum_{i\in I,J}\sum_{i>j\in I,J}\frac{1}{|\mathbf{r}_i-\mathbf{r}_j|}$$

$$H_I\Psi_I = E_I\Psi_I$$

$$H_{IJ}\Psi_{IJ} = E_{IJ}\Psi_{IJ}$$

$$E = \sum_{I>J}E_{IJ} - (N-2)\sum_I E_I$$

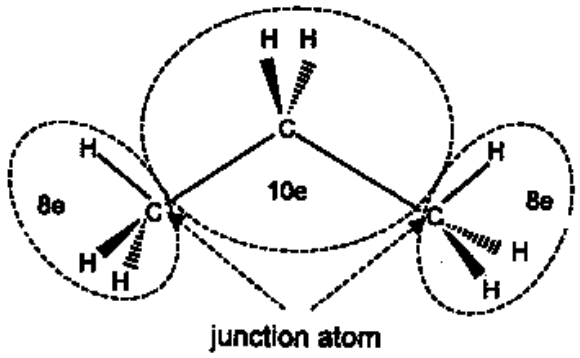

Fig. 1. Partition of molecule and electron assignment to fragments.

Consideration of electrostatic potentials arising from all the surrounding fragments

Accuracy of FMO method is excellent !

Polypeptides and proteins

Table Total energies of Alpha-1 and crambin

Molecule	PDB	Number of Residues	Total energy / a.u.		Error / kcal/mol
			FMO-HF/STO-3G	HF/STO-3G	
Alpha-1 (chain A)	3AL1	13	-4855.2759231	-4855.2754720	-0.3
Alpha-1 (chain B)	3AL1	13	-4855.5709689	-4855.5700528	-0.6
Alpha-1 (dimer)	3AL1	26	-9711.1897149	-9711.1883710	-0.8
[Pro^{22}, Leu^{25}]crambin	1EJG	46	-17779.5030137	-17779.5023991	-0.4
[Ser^{22}, Ile^{25}]crambin	1EJG	46	-17777.1487290	-17777.1483655	-0.2

Errors are confined within 1 kcal/mol.

Electron Correlations

Electron correlations play important roles for the descriptions of weak molecular interactions associated with hydrogen bonding and van der Waals (dispersion) forces.

- Watson-Crick pair
- Ligand binding
- DNA base stacking

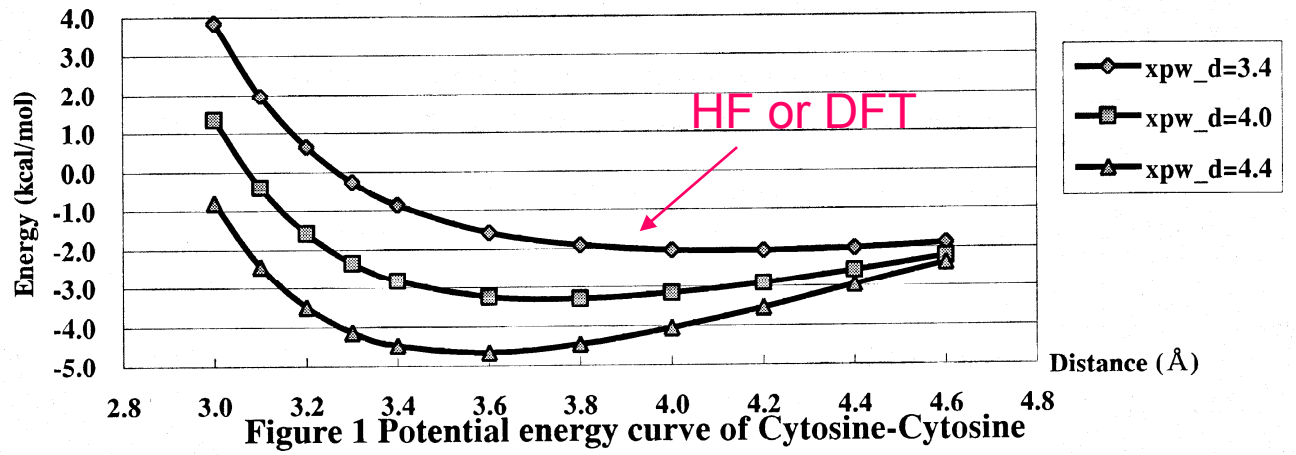

Figure 1 Potential energy curve of Cytosine-Cytosine

→ **FMO-MP2 or MP3 calculations on ABINIT-MPX software**

FMO calculations with MP2 and MP3

$$E^{MP2(2p-2h)} = \frac{1}{4}\sum_{ijab}\frac{\langle ij \| ab\rangle\langle ab \| ij\rangle}{\varepsilon_i + \varepsilon_j - \varepsilon_a - \varepsilon_b}$$

$$E_{MP2} = E^{MP2(2p-2h)}$$

$$E^{MP3(4p-2h)} = \frac{1}{8}\sum_{ijabcd}\frac{\langle ij \| ab\rangle\langle ab \| cd\rangle\langle cd \| ij\rangle}{(\varepsilon_i + \varepsilon_j - \varepsilon_a - \varepsilon_b)(\varepsilon_i + \varepsilon_j - \varepsilon_c - \varepsilon_d)}$$

$$E^{MP3(2p-4h)} = \frac{1}{8}\sum_{ijklab}\frac{\langle ij \| ab\rangle\langle ab \| kl\rangle\langle kl \| ij\rangle}{(\varepsilon_i + \varepsilon_j - \varepsilon_a - \varepsilon_b)(\varepsilon_k + \varepsilon_l - \varepsilon_a - \varepsilon_b)}$$

$$E^{MP3(3p-3h)} = \sum_{ijkabc}\frac{\langle ij \| ab\rangle\langle kb \| cj\rangle\langle ac \| ik\rangle}{(\varepsilon_i + \varepsilon_j - \varepsilon_a - \varepsilon_b)(\varepsilon_i + \varepsilon_k - \varepsilon_a - \varepsilon_c)}$$

Cost for MP3 is higher by
- ⇒ 8-10 times @ PC cluster
- ⇒ less than 2 times @ ES2 (efficient vectorization)

- integral direct
- DGEMM

$$E_{MP3} = E^{MP2(2p-2h)} + E^{MP3(2p-4h)} + E^{MP3(4p-2h)} + E^{MP3(3p-2h)}$$

(Y. Mochizuki *et al.*, Chem. Phys. Lett. 493 (2010) 346.)

MP2.5 Approximation

Scaled MP3 Non-Covalent Interaction Energies Agree Closely with Accurate CCSD(T) Benchmark Data

Michal Pitoňák,[a] Pavel Neogrády,[b] Jiří Černý,[a] Stefan Grimme,*[c] and Pavel Hobza*[a]

Chem. Phys. Chem. **10** (2009) 282

Scaled MP3 interaction energies calculated as a sum of MP2/CBS (complete basis set limit) interaction energies and scaled third-order energy contributions obtained in small or medium size basis sets agree very closely with the estimated CCSD(T)/CBS interaction energies for the 22 H-bonded, dispersion-controlled and mixed non-covalent complexes from the S22 data set. Performance of this so-called MP2.5 (third-order scaling factor of 0.5) method has also been tested for 33 nucleic acid base pairs and two stacked conformers of porphine dimer. In all the test cases, performance of the MP2.5 method was shown to be superior to the scaled spin-component MP2 based methods, e.g. SCS–MP2, SCSN–MP2 and SCS(MI)–MP2. In particular, a very balanced treatment of hydrogen-bonded compared to stacked complexes is achieved with MP2.5. The main advantage of the approach is that it employs only a single empirical parameter and is thus biased by two rigorously defined, asymptotically correct ab-initio methods, MP2 and MP3. The method is proposed as an accurate but computationally feasible alternative to CCSD(T) for the computation of the properties of various kinds of non-covalently bound systems.

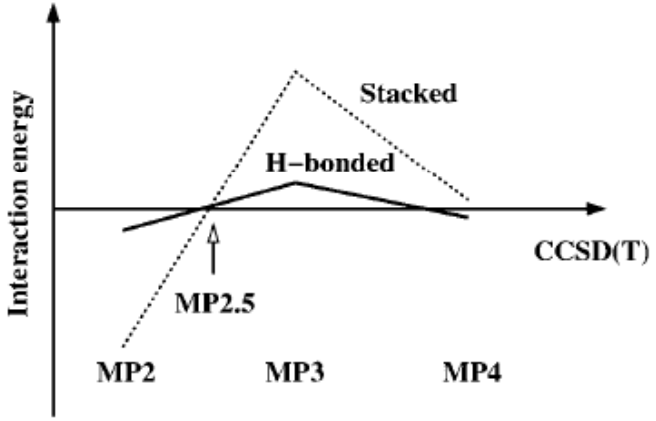

$$E(MP2.5) = E(MP2) + 0.5\, E^{corr}(MP3)$$

$$E(MP2.5/large\ basis) \doteqdot E(MP2/large\ basis) + \Delta E(MP2.5\text{-}MP2/small\ basis)$$

Comparable accuracy to CCSD(T)

BSSE and CP correction

$$E^{\mathrm{FMO}} = \sum_{I}^{N} E_I + \sum_{I>J}^{N} (E_{IJ} - E_I - E_J)$$
$$= \sum_{I}^{N} E'_I + \sum_{I>J}^{N} \Delta\widetilde{E}_{IJ}$$

$$\Delta\widetilde{E}_{IJ} = E'_{IJ} - E'_I - E'_J + \mathrm{Tr}\left(\Delta\mathbf{P}^{IJ}\mathbf{V}^{IJ}\right) \quad \text{IFIE}$$

where $\Delta\mathbf{P}^{IJ}$, $\mathbf{V}^{IJ}$, E'_I, E'_{IJ} are the difference matrix of electron density, the environmental ESP for dimer, and the energies of monomer and dimer without the environmental ESP, respectively.

$$\delta E_1^{(1\cup2)} = E_1^{(1)} - E_{1[2]}^{(1\cup2)}$$

$$\delta E_2^{(1\cup2)} = E_2^{(2)} - E_{2[1]}^{(1\cup2)},$$

$$\delta E_{12}^{\mathrm{BSSE}} = \delta E_1^{(1\cup2)} + \delta E_2^{(1\cup2)} = E_1^{(1)} + E_2^{(2)} - E_{1[2]}^{(1\cup2)} - E_{2[1]}^{(1\cup2)}$$

Case study: ER-EST complex

Estrogen Receptor

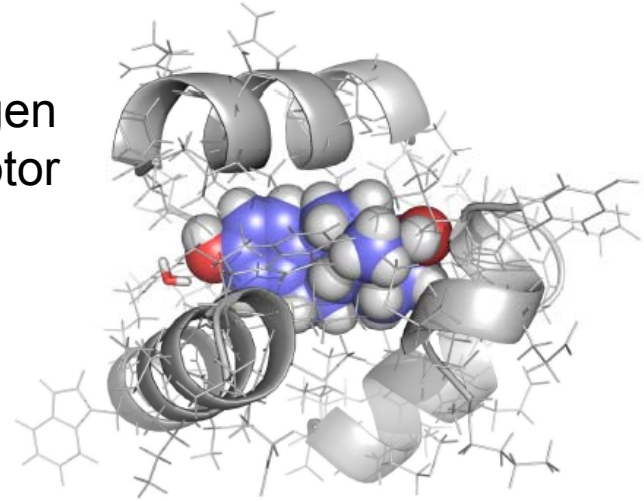

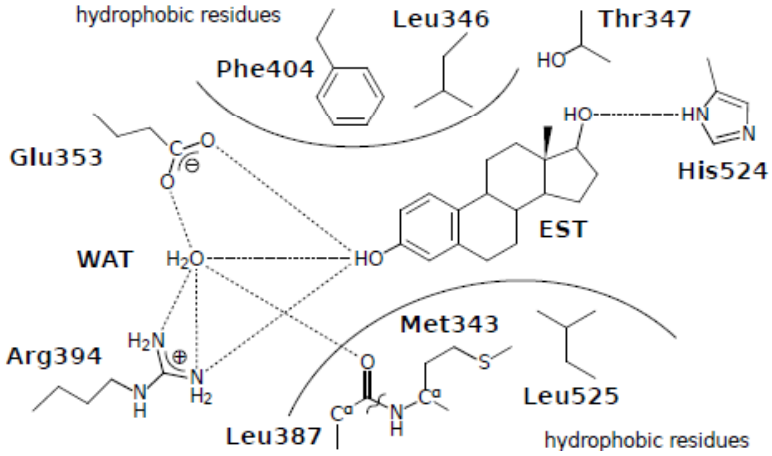

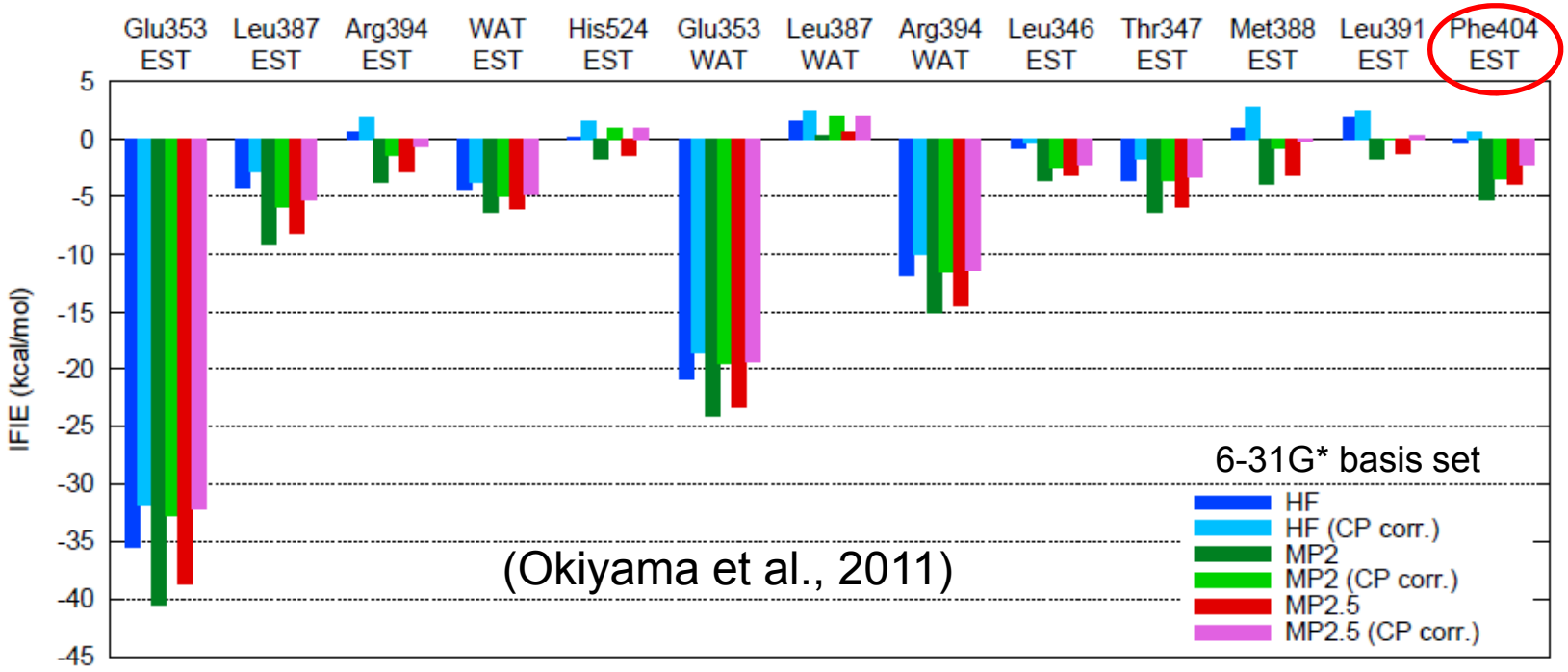

Structure of Influenza Virus

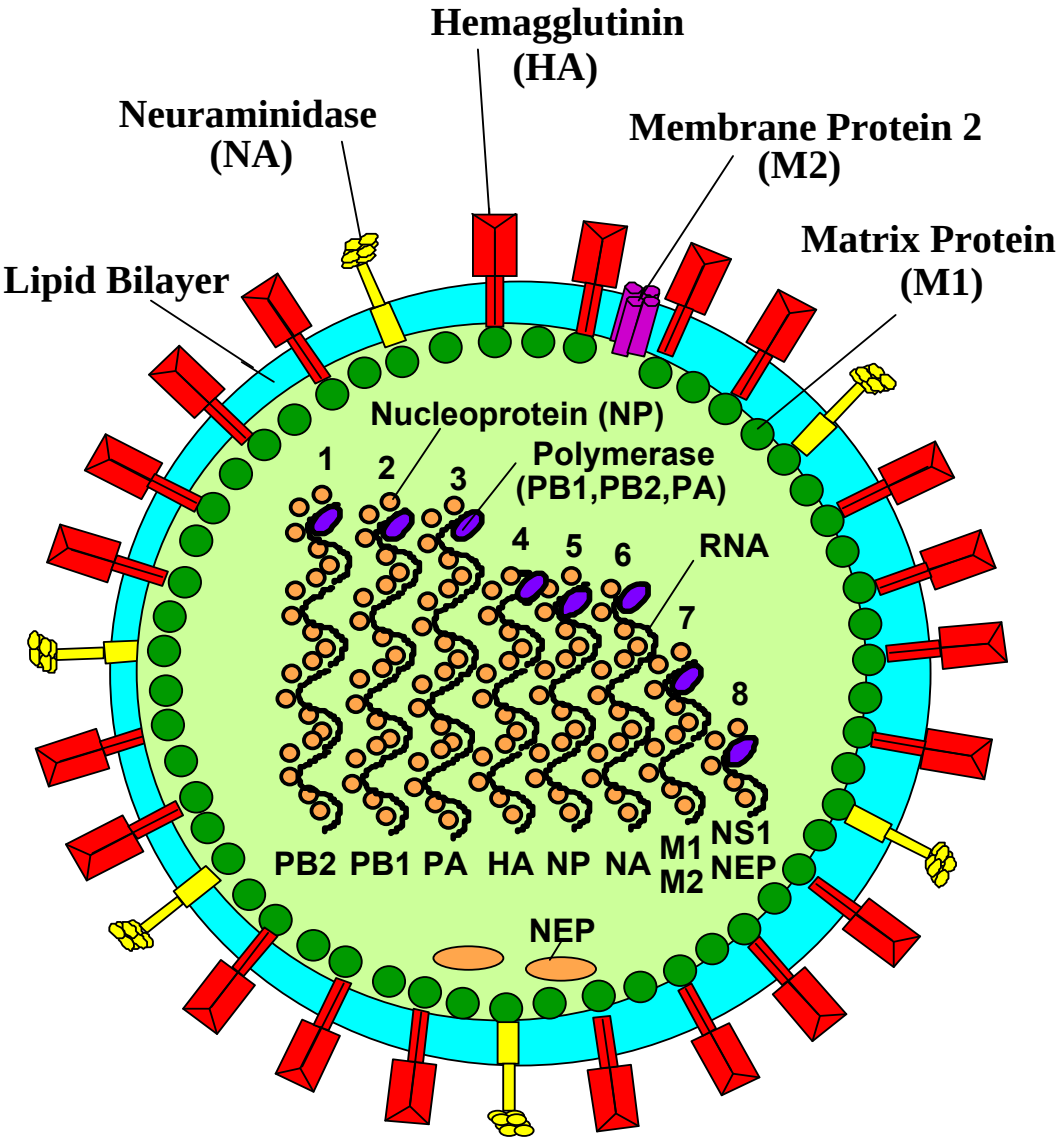

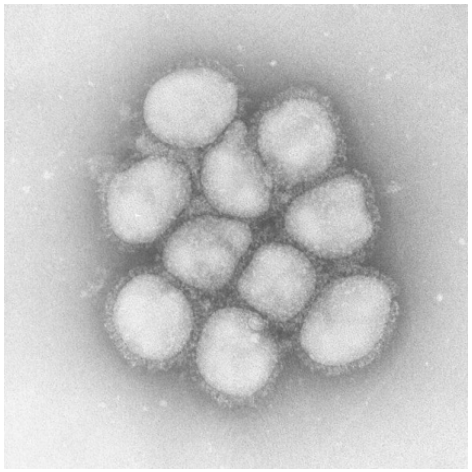

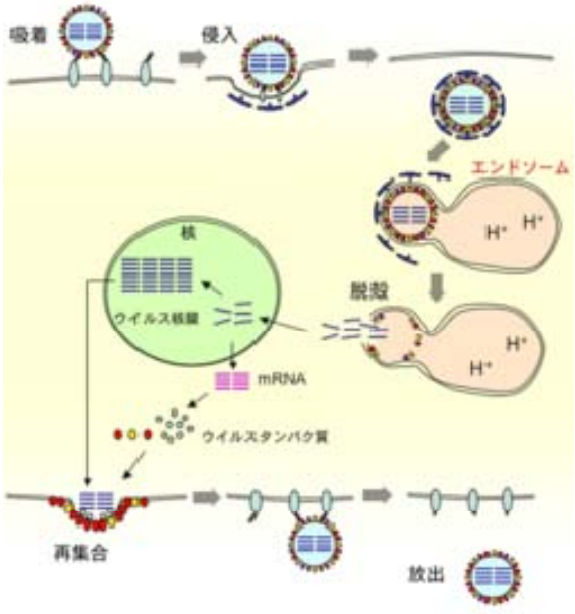

Host cell invasion and replication by influenza virus

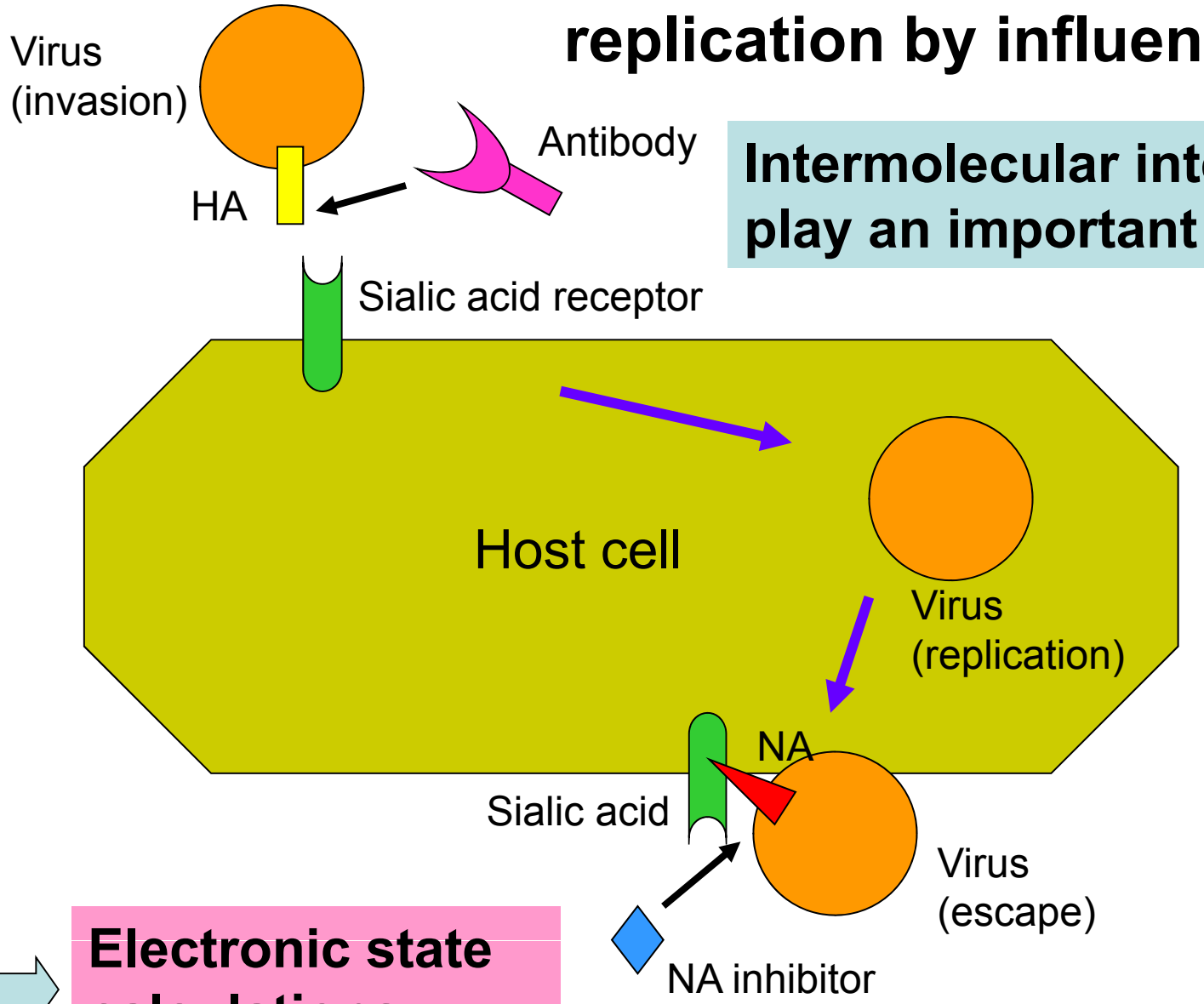

Intermolecular interactions play an important role.

Electronic state calculations

FMO-MP2 calculation for influenza hemagglutinin antigen-antibody system with ABINIT-MPX

- Influenza Hemagglutinin (HA) Protein Complex with Fab Fragment (1EO8)
  ⇒ Antigen : HA1(green)、HA2(red)
  Antibody : H chain(pink)、L chain(yellow)
- World's largest FMO-MP2/6-31G calculation
  ⇒ 921 residues、14,086 atoms
  78,390 Aos
- Benchmark on PC cluster
  (Opteron 2GHz, 16 processors)
  ⇒ 198.9 hours (8.3 days)
- Benchmark on Earth Simulator
  (512 nodes, 4,096 processors)
  ⇒ 53.4 minutes !
- MP2-IFIE analysis
  ⇒ Molecular recognition mechanism

1EO8: H3N2 A/Aichi/68

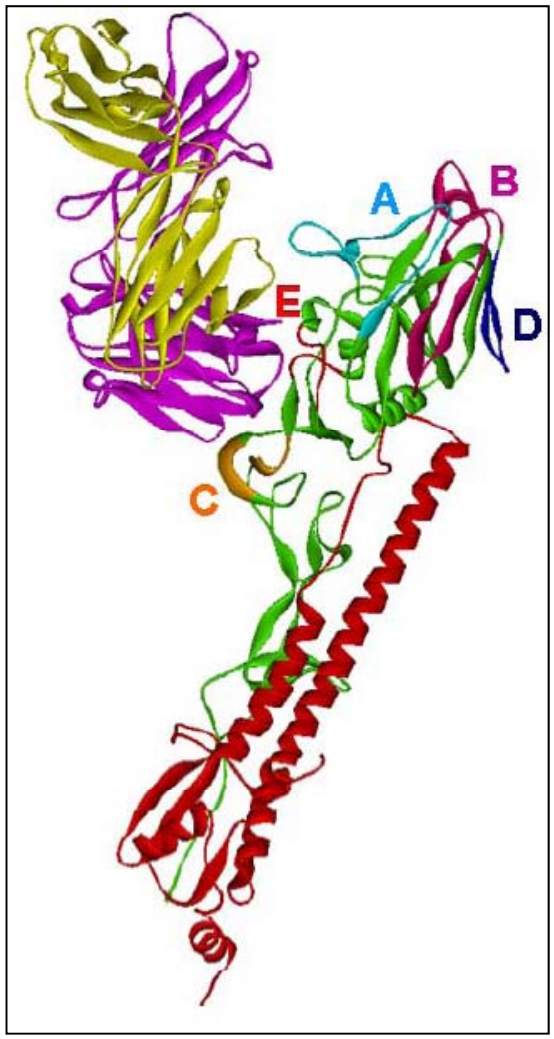

A-E: Antigenic regions

(Y. Mochizuki *et al*., Chem. Phys. Lett. 457 (2008) 396.)

Criterion for Probable Mutations

For the mutation in HA to take place, it should satisfy the two conditions:

1) After the mutation, that HA should preserve the function for the infection into host cell. This property can be evaluated in terms of the hemadsorption experiment by amino acid substitution, in which the hemadsorption activity of mutant associated with the binding to sialic acid moieties on the host cell is measured.

2) The amino acid site at which the residue is substantially attracted by the antibody would be preferentially mutated to escape the antibody pressure.

The residues to satisfy these two conditions would have a high probability of the mutation.

Prediction of antigenic variations

Possible HA variants with mainstream amino acid changes require following conditions:

1. Maintain function of HA
HA variant with random one-point amino acid change should preserve **hemadsorption activity**. (i.e. binding activity to sialic acid.)

2. Have lower affinity with antibody
Based on the **FMO-IFIE analysis**, interaction strength between antibody and each amino acid of HA is quantitatively estimated.
⇒ amino acid with **attractive interaction to antibody** would be changed to escape antibody pressure.

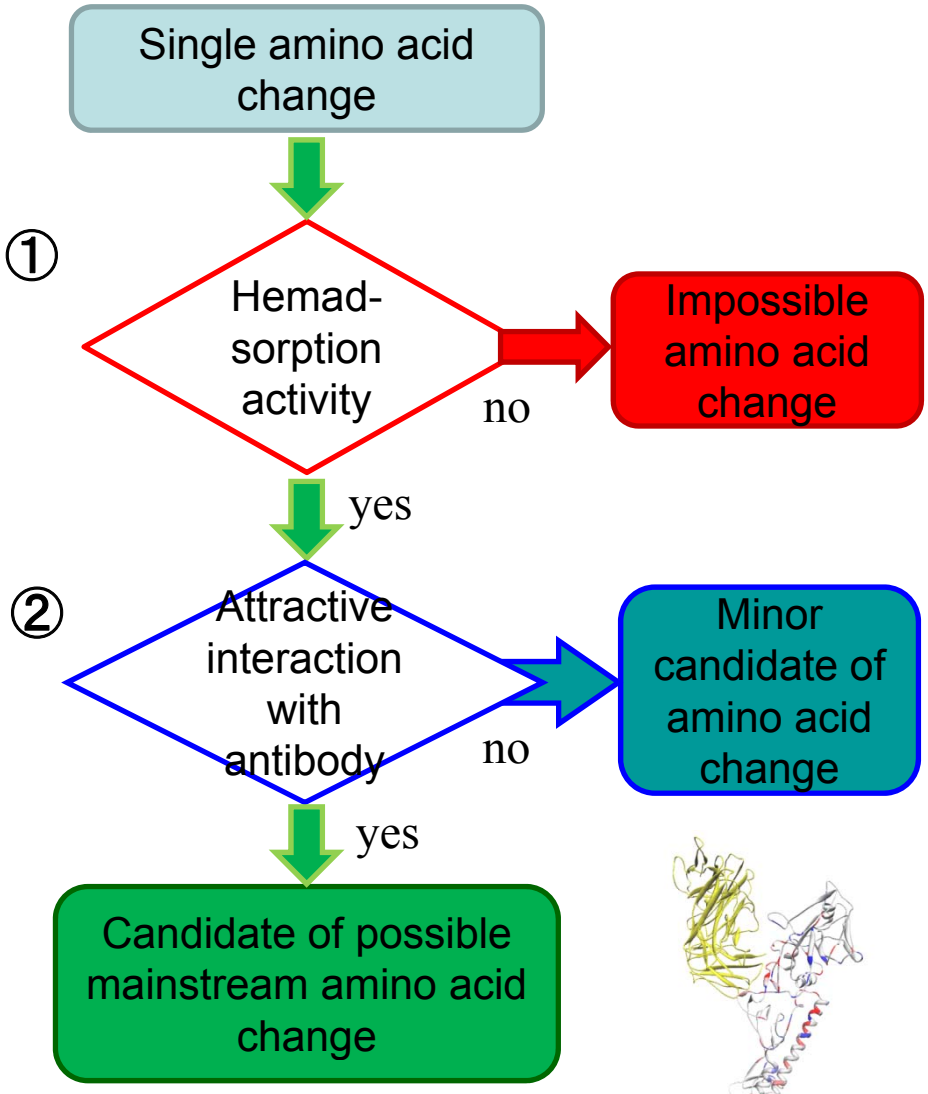

Antigen-antibody interactions and prediction of antigenic variations

History of amino acid changes for H3HA (A/Aichi/68)

- 1969 • V78G
- 1972 • D63N ※
- 1973 • T83K
- 1977 • I62K
- 1987 • E82K
- 1989 • K83E
- 1995 • K62E
- 2002 • H75Q
- 2002 • E83K

Mainstream amino acid changes of the H3 HA1 (A/Aichi/68) at the antigenic region E (year 1968 – 2002).

Antigenic region E

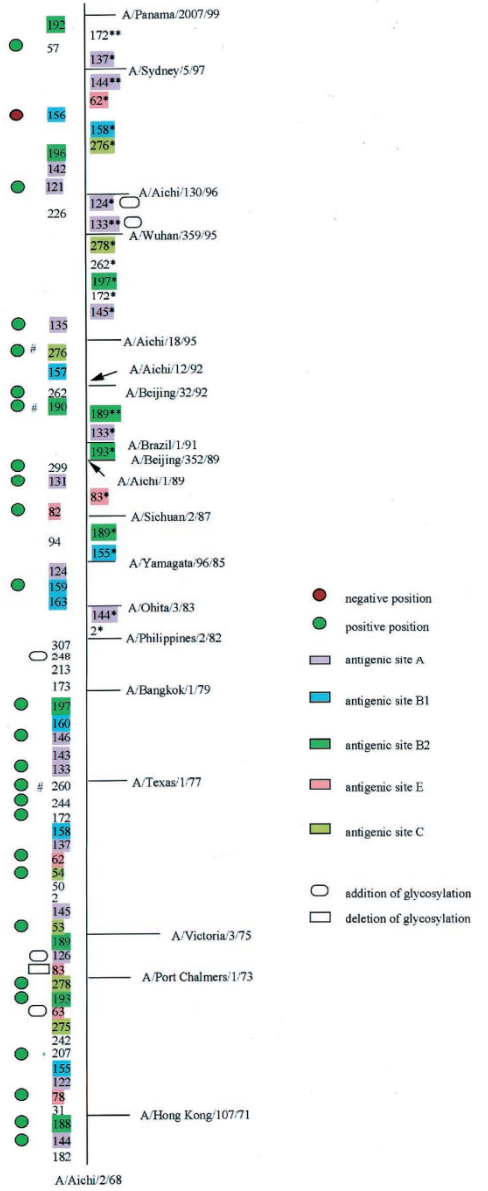

※Hemadsorption experimental data is not available.

K. Nakajima et al., J. Virol. 77 (2003) 10088.

Comparison to mutation history

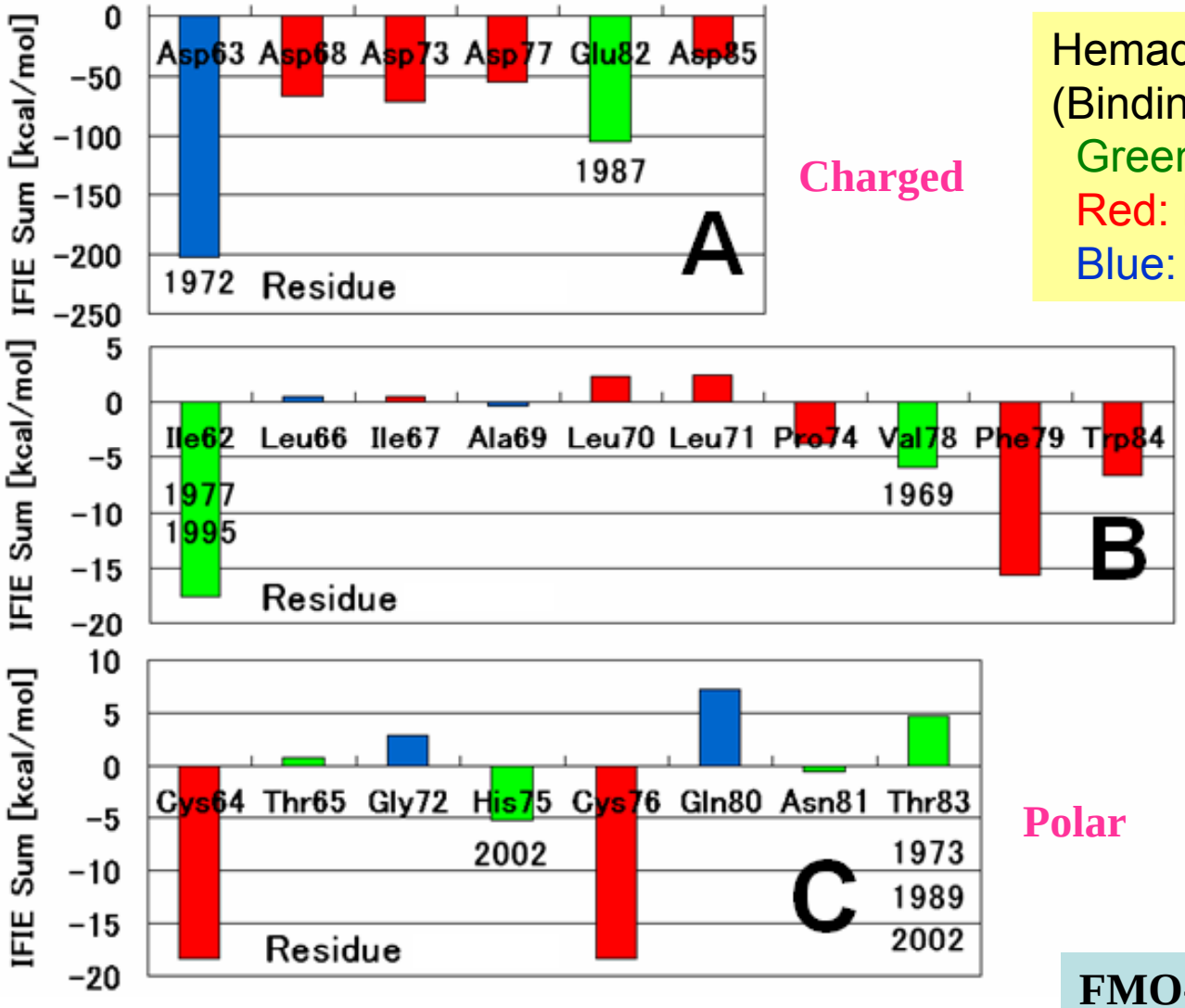

Charged

Hydrophobic

Polar

Hemadsorption Experiment
(Binding Ability to Host Cell)
Green: Allowed
Red: Prohibited
Blue: No Data

FMO-MP2/6-31G*

(K. Takematsu *et al.*, J. Phys. Chem. B 113 (2009) 4991.)

Recent Studies by FMO-MP2 and MP3

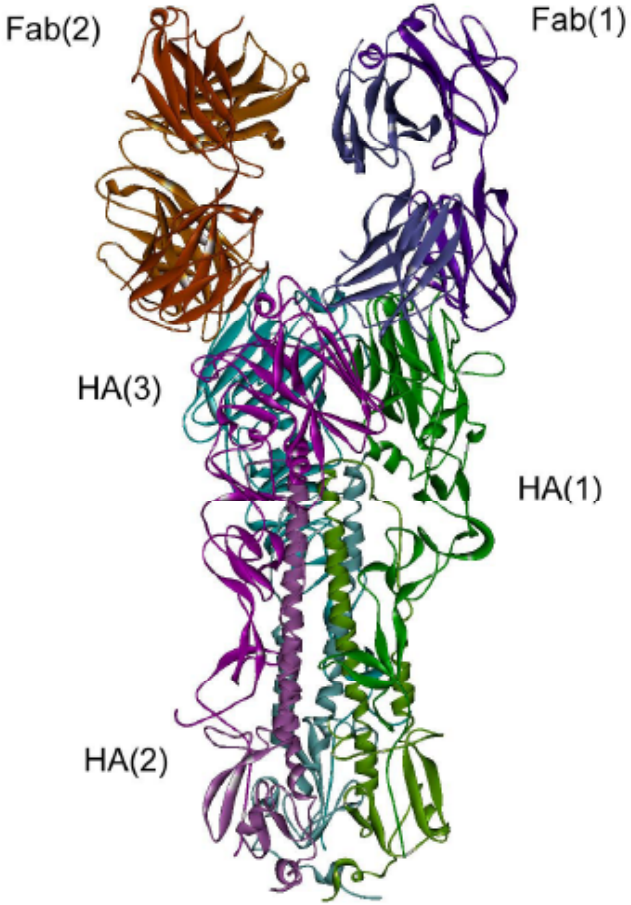

HA trimer – Fab antibody (1KEN; 2351 residues)

H3N2

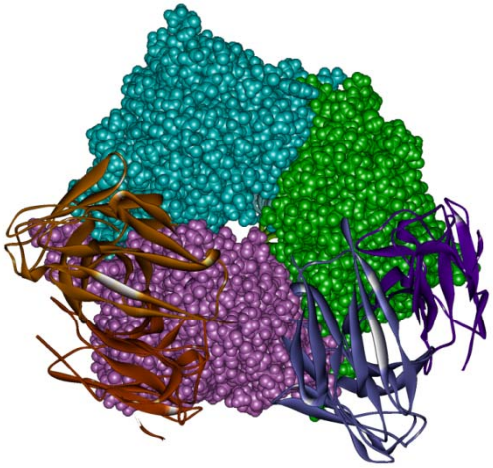

(Top view)

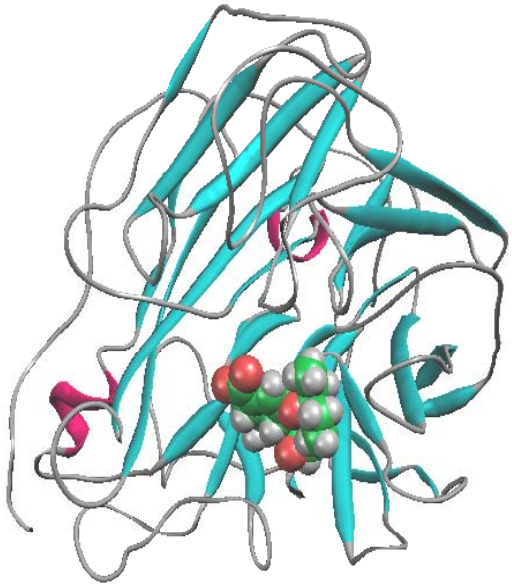

NA – oseltamivir (2HU4;386 residues)

H5N1

FMO calculations by ABINIT-MPX on Earth Simulator (ES2)

Hybrid Parallelization with MPI-OpenMP

- Inter-fragment: MPI; Intra-fragment: OpenMP

  ⇒ Hybrid parallelization

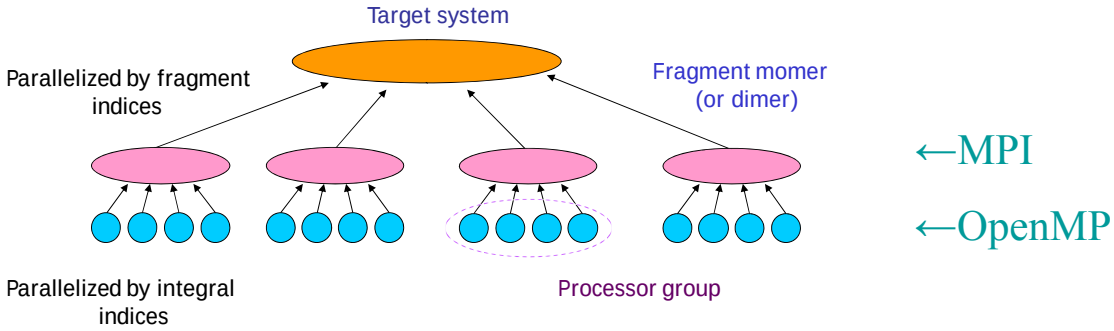

- Memory saving by sharing MP3 arrays among threads

  ⇒ OpenMP is promising for acceleration on multi-core chips

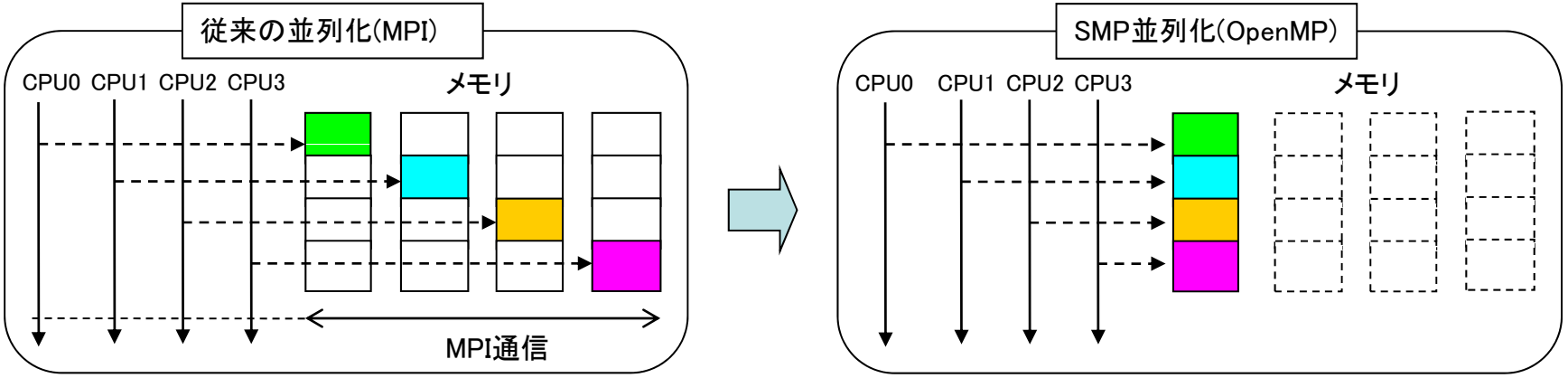

ES2 was used as a massively parallel-vector computational platform.

Computation time on ES2

SYSTEM	LEVEL	NODES	TIME(h)	(MP3/2)	NODE RAT.	TFLOPS
HA1	FMO-MP2	64	1.7			0.97
	FMO-MP3	64	2.7	(x1.6)		2.27
	FMO-MP2*	64	4.4			1.19
	FMO-MP3*	64	8.7	(x2.0)		3.02
	FMO-MP2	128	0.8		2.1	2.06
	FMO-MP3	128	1.3	(x1.6)	2.1	4.67
HA3	FMO-MP2	64	9.4			0.83
	FMO-MP3	64	11.9	(x1.3)		1.66
	FMO-MP2	128	4.3		2.2	1.83
	FMO-MP3	128	5.8	(x1.3)	2.1	3.44
NA	FMO-MP3	64	1.0			3.04
	FMO-MP3*	64	4.4			3.09

- 64 nodes = 512VPUs, 6-31G or 6-31G* basis set, Cys-Cys = 1 fragment
- HA1 (14086 atoms, 921 residues, 78390 AOs for 6-31G, 121314 AOs for 6-31G*)
- HA3 (36160 atoms, 2351 residues, 201276 AOs for 6-31G)
- NA (5792 atoms, 386 residues, 32549 AOs for 6-31G, 50447 AOs for 6-31G*)

Inter-domain interactions in HA trimer system

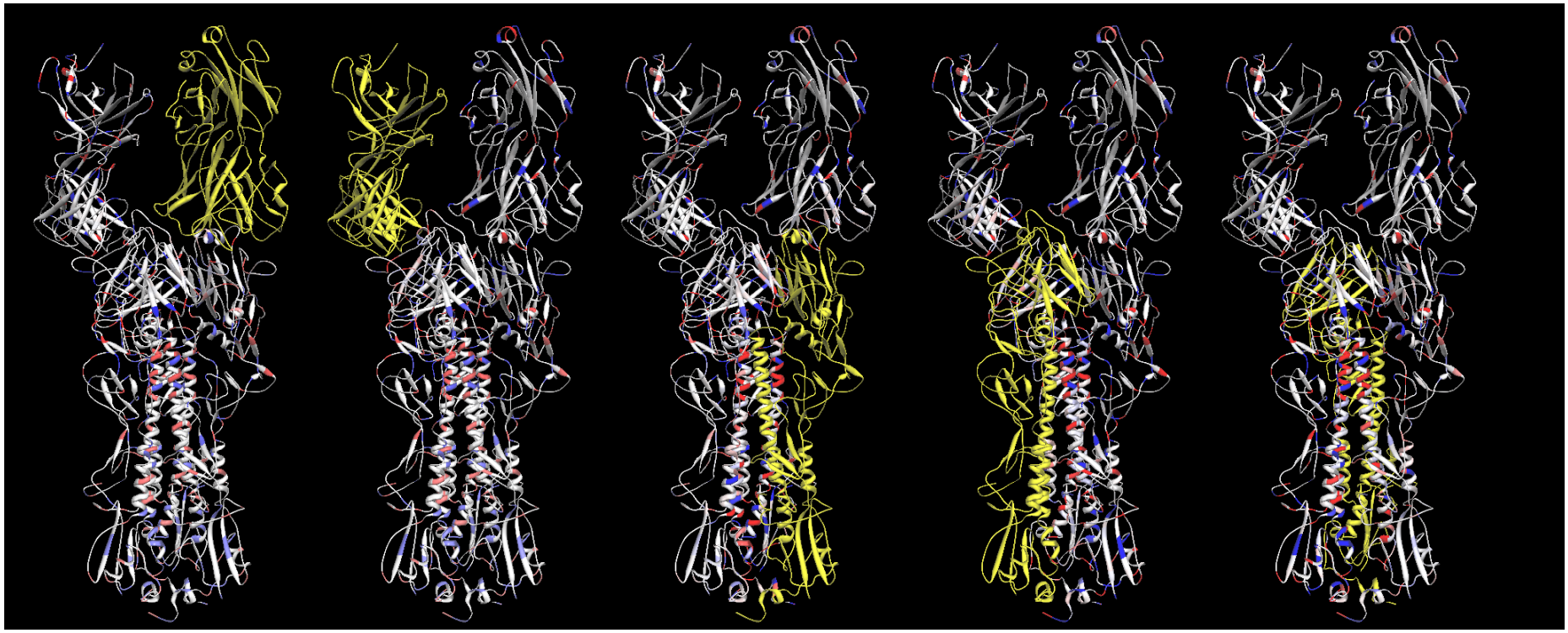

IFIEs between yellow part and each amino acid residue

IFIE sum (kcal/mol)

Domains	HF	MP2	MP3
Fab(I):HA(I)	-288.8	-367.0	-352.8
Fab(I):HA(II)	177.5	155.6	158.7
Fab(I):HA(III)	134.3	134.2	134.3
Fab(II):HA(I)	137.0	137.0	137.0
Fab(II):HA(II)	-292.7	-380.4	-363.7
Fab(II):HA(III)	170.8	157.0	159.5

Domains	HF	MP2	MP3
HA(I):HA(II)	-1022.4	-1280.3	-1237.1
HA(II):HA(III)	-981.7	-1245.7	-1200.6
HA(I):HA(III)	-1189.0	-1469.8	-1421.3
Fab(I):Fab(II)	210.8	197.8	199.5
HA:Fab	**38.1**	**-163.6**	**-127.0**

Results for HA trimer – antibody complex

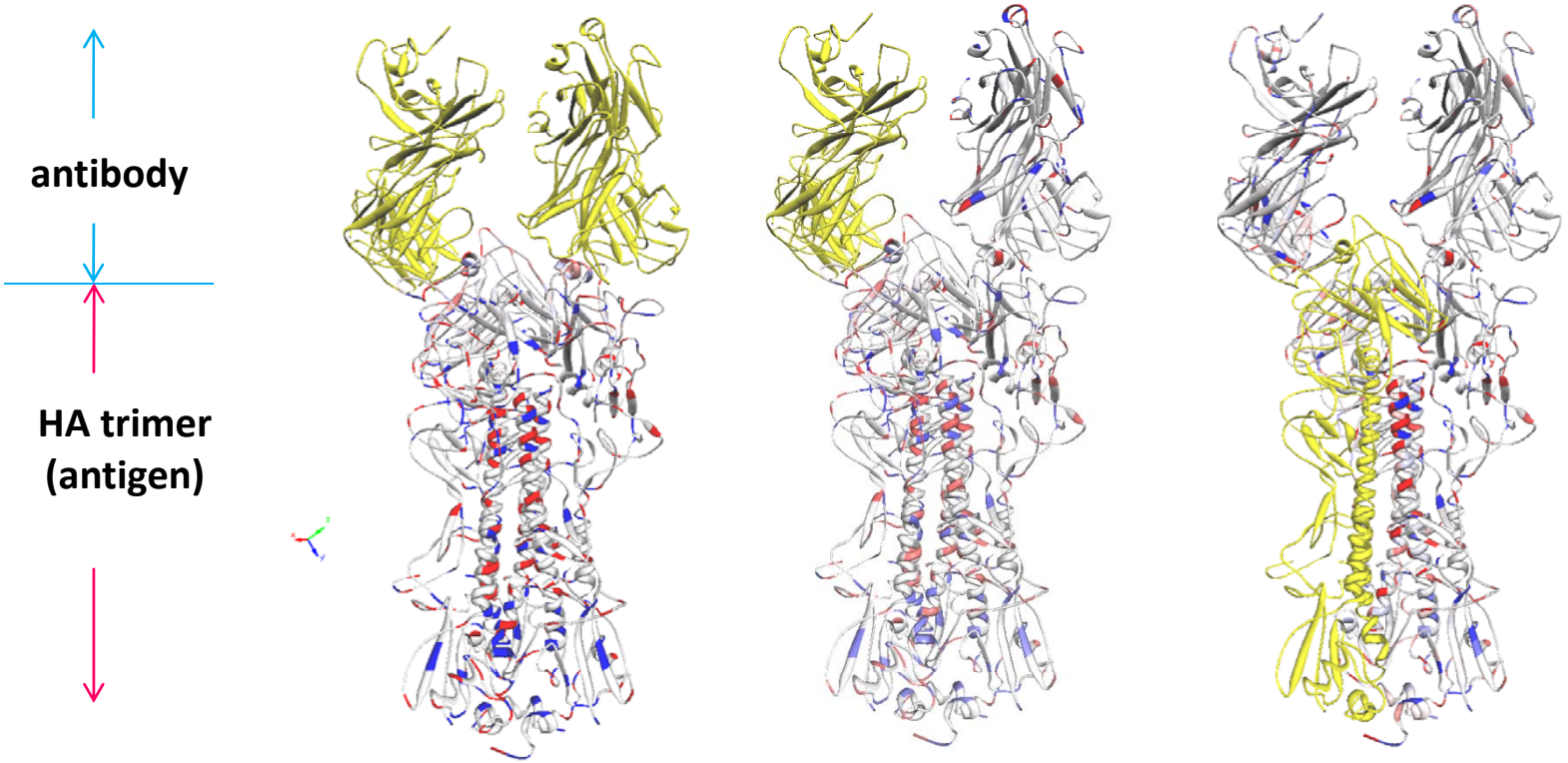

FMO-MP3/6-31G

- Left figure:
  Residues in red ⇒ Attractive interaction with antibody (yellow)
  Residues in blue ⇒ Repulsive interaction with antibody (yellow)
- Mutation of red residues would facilitate the escape from antibody pressure.
  ⇒ Prediction of mutations and development of vaccines
- Middle and right figures:
  Domain-domain interactions ⇒ Trimer functions ?

Prediction based on HA trimer

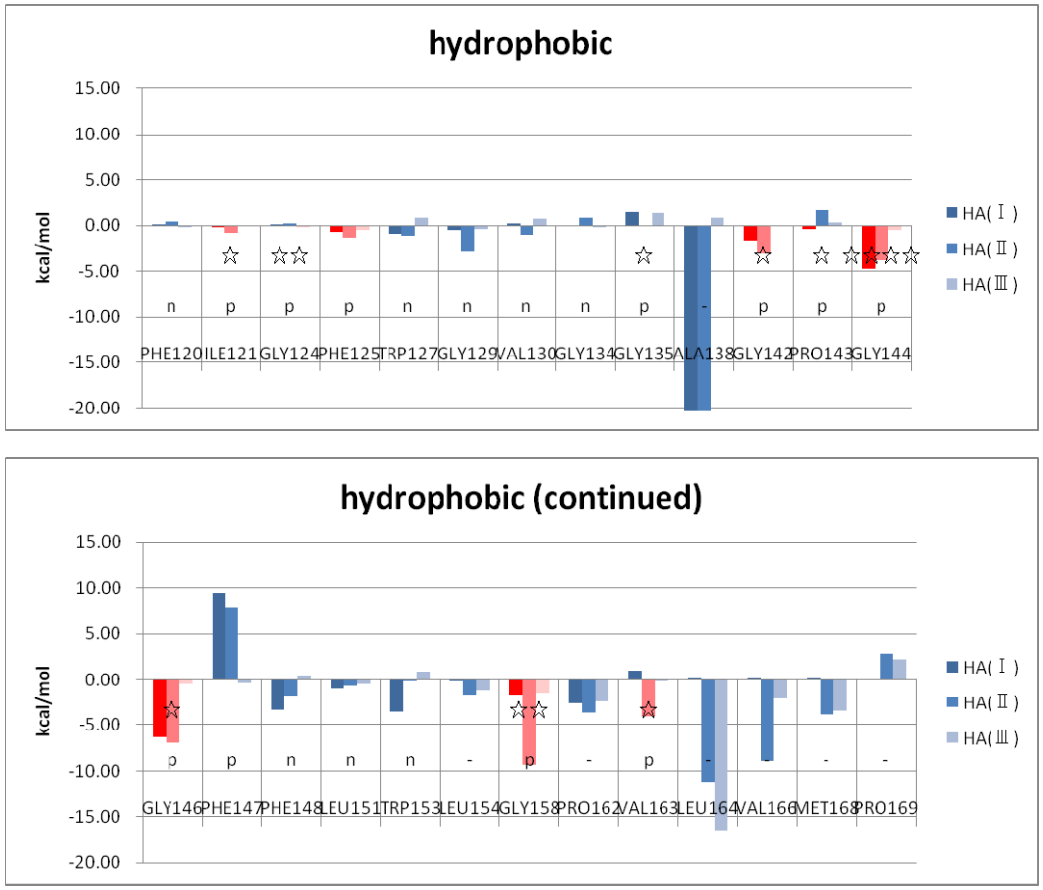

* Good correlation between theoretical prediction (red, allowed & attractive) and historical fact for mutations (star)
* Fluctuations in interactions between antibody and residue in HA trimer

Results for NA with oseltamivir

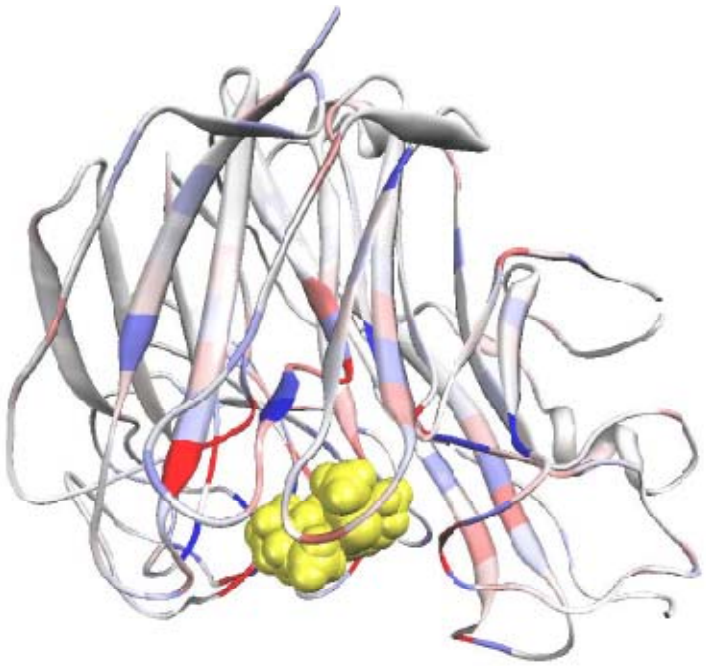

(Yellow: oseltamivir)

- Oseltamivir: inhibitor to NA

- Amino acid residues in red
  ⇒ Attractive interactions with oseltamivir

  Amino acid residues in blue
  ⇒ Repulsive interactions with oseltamivir

- Drug resistance may be acquired if the residues in red are mutated.
  ⇒ Prediction of mutations

- More effective inhibitors can be designed by adjusting the interactions with red and blue residues.
  ⇒ Rational drug design

NA-oseltamivir complex

(M. Tsuboi)

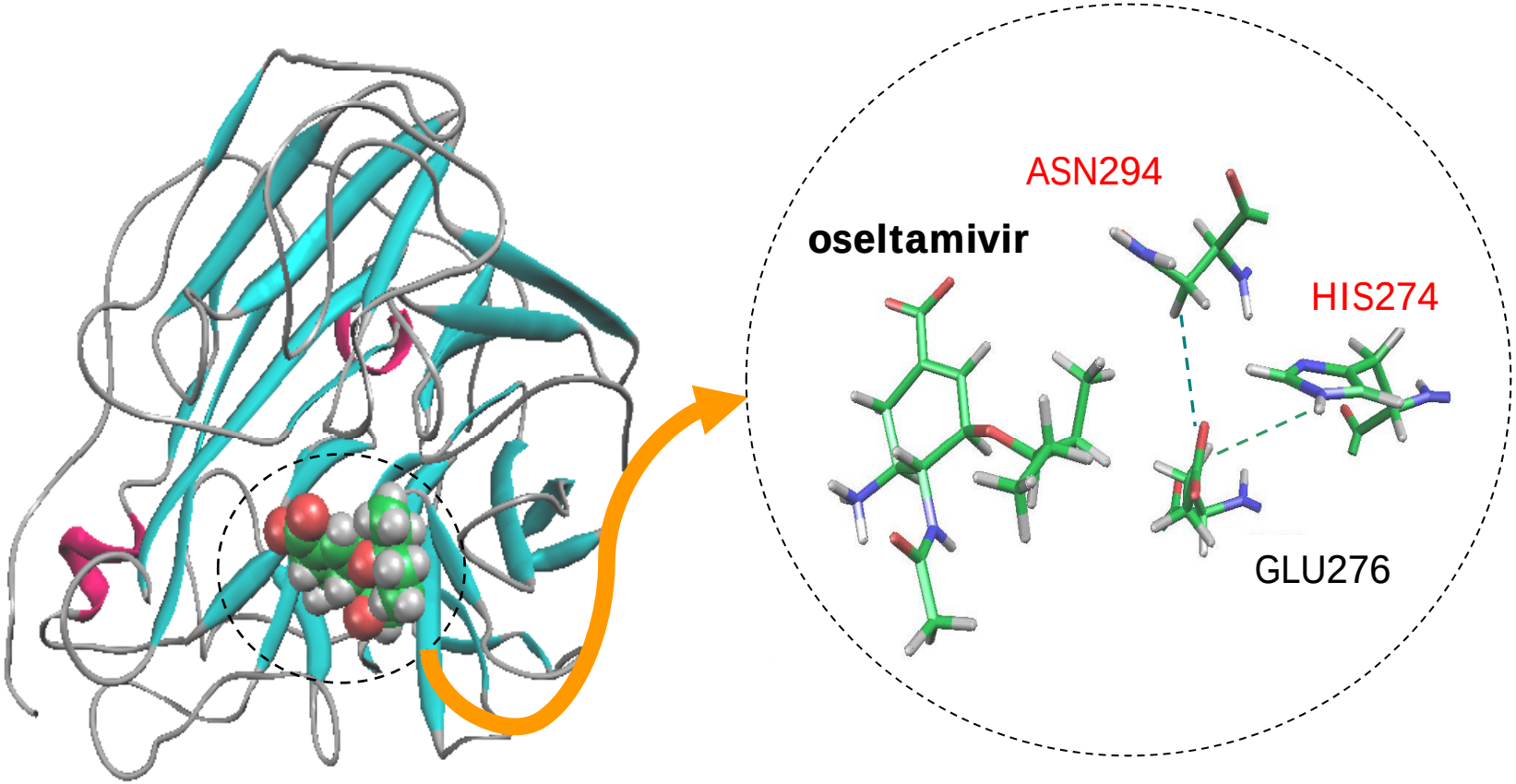

Wild Type

Ligand binding pocket

Mutations for resistance against oseltamivir

FMO2-MP2/6-31G

Wild Type

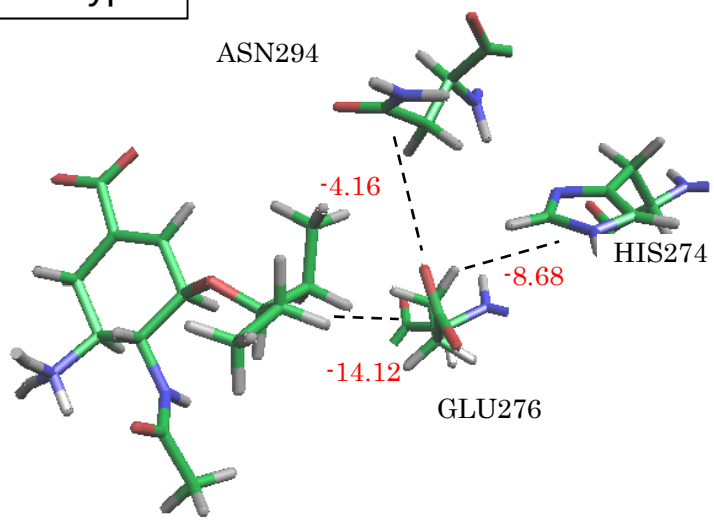

HIS274TYR

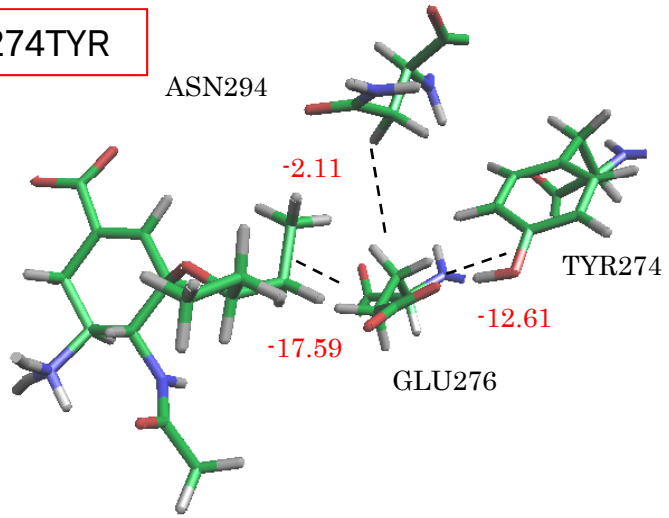

ASN294SER

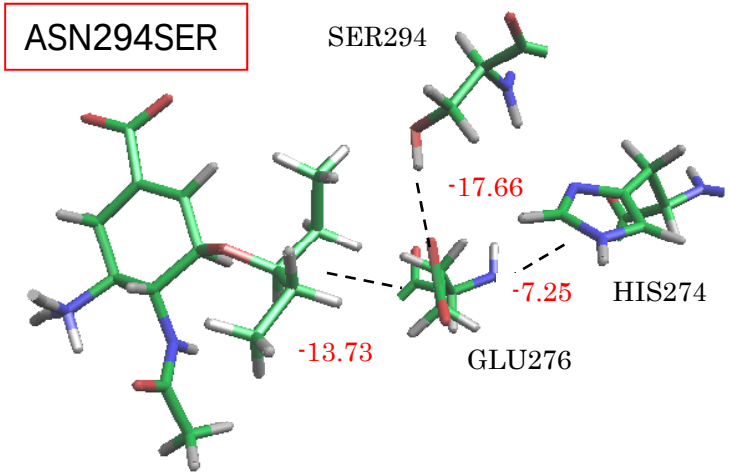

Red values ・・・IFIE(kcal/mol)

$$IFIE-SUM=\sum_{I}\Delta E_{LI}$$

		Wild Type	His274Tyr	Asn294Ser
IFIE-SUM	(kcal/mol)	-321.31	-318.80	-321.12
Expt.(inhibition)		1	265	81

Comparison between calculation and experiment

Calculated results are consistent with binding experiments.

FMO Calculations for Gound State

- Ab initio FMO calculations were carried out for influenza HA and NA proteins complexed with antibody or inhibitor.
- High-speed, parallelized MP2 and MP3 calculations were performed on ES2.
- Quantitative information on inter-fragment interactions in these systems would provide useful tools for mutation prediction and drug design for influenza viruses.

Bioluminescence Spectra of Firefly

Excited state calculations by FMO

High quantum yield (approx. 90 % ?)

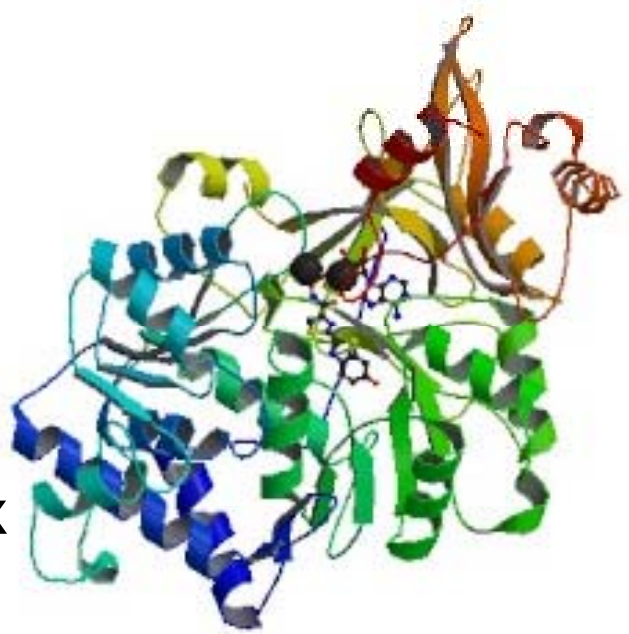

Luciferase-oxyluciferin complex
(*Luciola cruciata*)

Color Tuning by ILE288

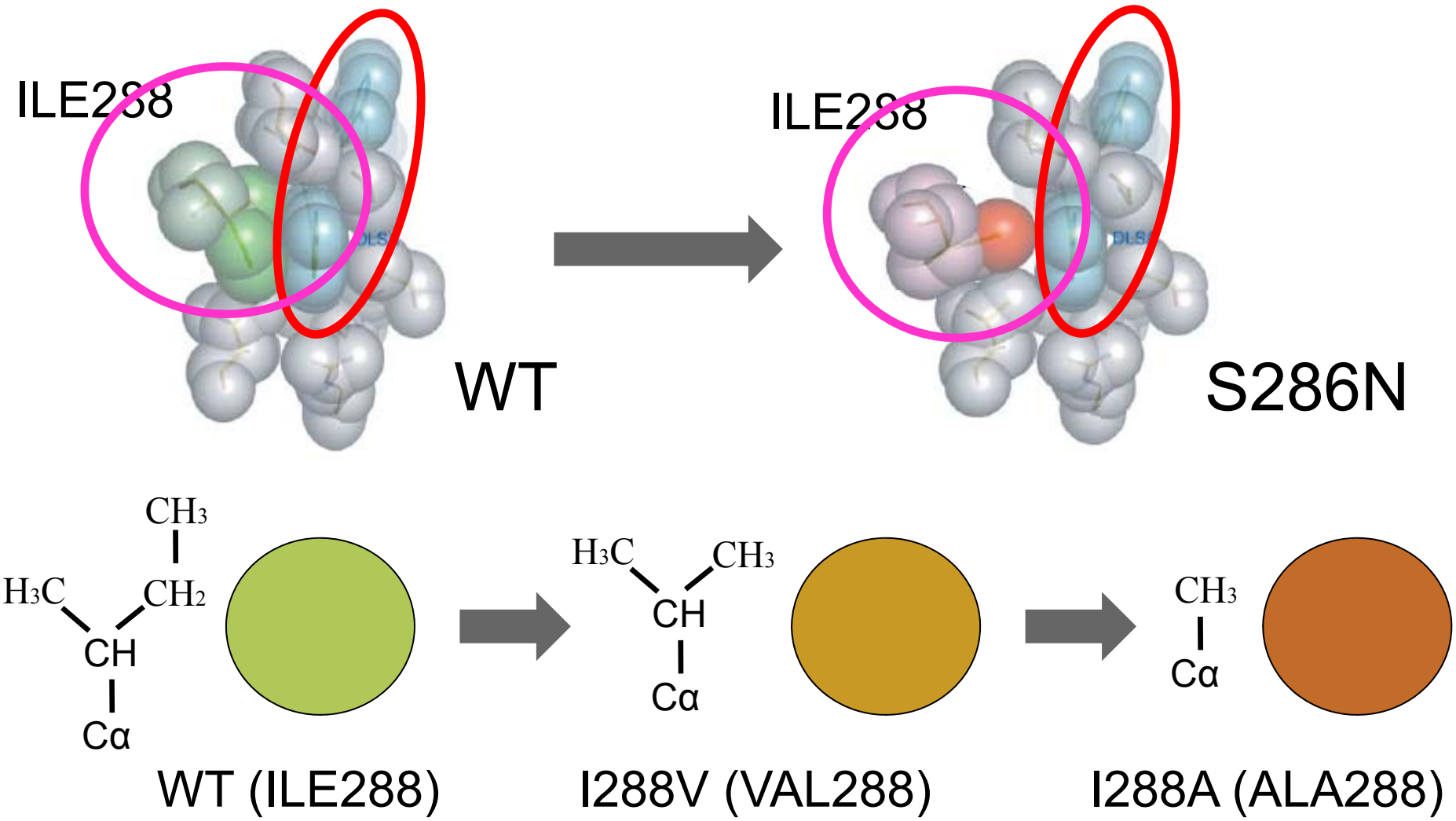

T. Nakatsu, S. Ichiyama, J. Hiratake, A. Saldanha, N. Kobashi, K. Sakata & H. Kato, *Nature* 440 (2006) 372.

Multi-Layer FMO (MLFMO) Method

$$E = \sum_{L_i}\left[\left(\sum_{I\in L_i} E'^{L_i}_I + \sum_{\substack{I>J \\ I,J\in L_i}} \Delta\widetilde{E}^{L_i}_{IJ}\right) + \sum_{L_j>L_i}\sum_{I\in L_i}\sum_{J\in L_j}\Delta\widetilde{E}^{L_i}_{IJ}\right]$$

Layer1

Layer2

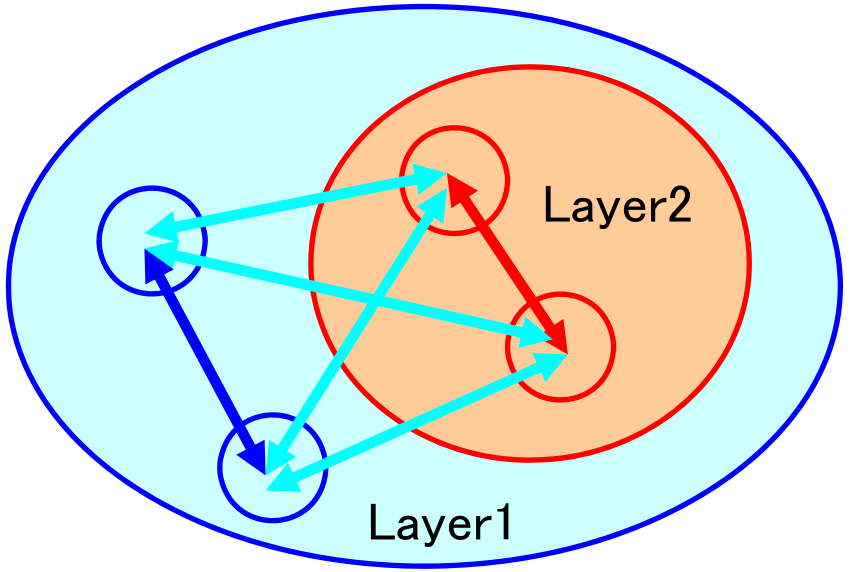

E_I : Monomer energy, E_{IJ} : Dimer energy

$$E_I = E'_I + Tr\left(\mathbf{D}^I\mathbf{V}^I\right), \quad E_{IJ} = E'_{IJ} + Tr\left(\mathbf{D}^{IJ}\mathbf{V}^{IJ}\right)$$

$$\Delta E'_{IJ} = E'_{IJ} - E'_I - E'_J, \quad \Delta\mathbf{D}^{IJ} = \mathbf{D}^{IJ} - \mathbf{D}^I \oplus \mathbf{D}^J$$

$$\Delta\widetilde{E}_{IJ} = \Delta E'_{IJ} + Tr\left(\Delta\mathbf{D}^{IJ}\mathbf{V}^{IJ}\right)$$

- Layer 2: Important region to which accurate (correlated) methods are applied.
- Layer 1 is analyzed by FMO-HF or MM (XUFF) method, while layer 2 is analyzed under the environmental electrostatic potentials by layer 1.
  - ⇒ MLFMO-MP2, MLFMO-CIS, MLFMO-CIS(D) methods available.

D.G. Fedorov and K. Kitaura, *J. Chem. Phys.* **122**, 054108 (2005).

Reproduction of experimental results

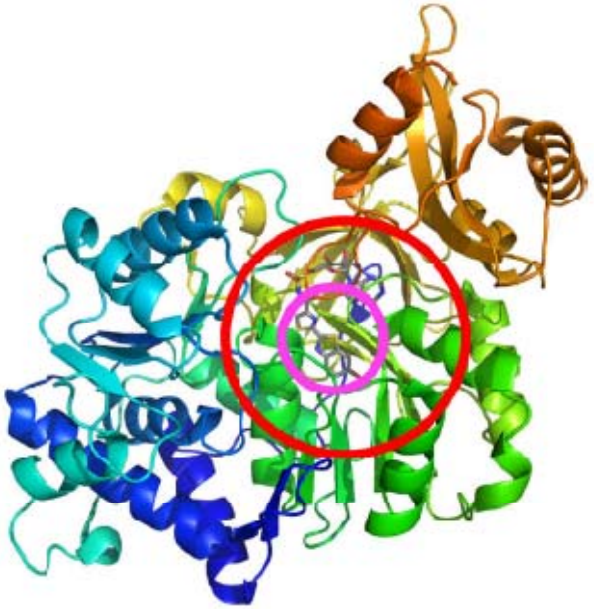

Fig. 2. Structure of luciferase (PDBID: 2D1S). Model 1 with the amino acid residues within the distance of 4.5 Å from oxyluciferin and AMP is included in red circle. Layer 2 is included in pink circle, while the other region corresponds to Layer 1.

(reduced size)

Table 2
Calculated values of emission energy and corresponding wavelength of WT and three mutant forms (model 1) obtained by MLFMO-CIS(D)/6-31G calculations in comparison with experimental values.

		WT	I288V	S286N	I288A
Emission energy (eV)	Calc.	2.49	2.49	2.39	2.37
	Expt.	2.21	2.02, 2.21	2.05	2.02
Wavelength (nm)	Calc.	498	498	518	523
	Expt.	560	560, 613	605	613
Color	Expt.	Yellow–green	Orange	Red	Red

(full size)

Table 5
Results of emission energy (eV) for WT and I288A with model 2 obtained by MLFMO-CIS(D)/6-31G and MLFMO-PR-CIS(Ds)/6-31G calculations in comparison with the experimental values. (A) Assigning only oxyluciferin to the Layer 2; (C) Assigning oxyluciferin, ILE288 (or ALA288), PHE249 and ALA350 to the Layer 2.

Layer 2	A		C		
Method	CIS(D)	PR-CIS(Ds)	CIS(D)	PR-CIS(Ds)	Expt.
WT	2.30	2.27	2.26	2.23	2.21
I288A	2.25	2.22	2.15	2.12	2.02

(A. Tagami *et al.*, Chem. Phys. Lett. 472 (2009) 118.)

Incorporation of Solvent Effects

Implicit Approach: Poisson-Boltzmann Equation

$$\nabla[\epsilon(\mathbf{r})\nabla\Psi(\mathbf{r})] = -\rho(\mathbf{r}) - \sum_i c_i z_i q \lambda(\mathrm{r}) \exp\left[\frac{-z_i q \Psi(\mathbf{r})}{k_\mathrm{B} T}\right]$$

where $\epsilon(\mathbf{r}), \Psi(\mathbf{r}), \rho(\mathbf{r}), c_i, z_i, q, k_\mathrm{B}, \lambda(\mathbf{r})$ are position-dependent dielectric function, electrostatic potential, charge density of solute, concentration of ion i, charge of the ion, charge of a proton, the Boltzmann constant, and a factor for the position-dependent accessibility to the ions in solution,

Table 1: Electrostatic contribution and non-polar contribution to solvation free energies (in kcal/mol) of polyalanines, where FMO-PB, MO-PB and classical PB mean the electrostatic contributions by each method.

	FMO-PB	MO-PB	Classical PB	Non-polar
ALA5 α-helix	186.7	188.4	187.4	2.9
ALA5 β-strand	162.2	163.2	160.2	3.4
ALA10 α-helix	268.5	269.1	238.5	4.4
ALA10 β-stand	212.2	213.7	195.1	6.2

(H. Watanabe *et al.*, Chem. Phys. Lett. 500 (2010) 116.)

FMO-ESP charge: Difference in ligand binding pocket of ER-EST

(a) $\Delta V = V_{\text{Mulliken}} - V_{\text{FMO}}$

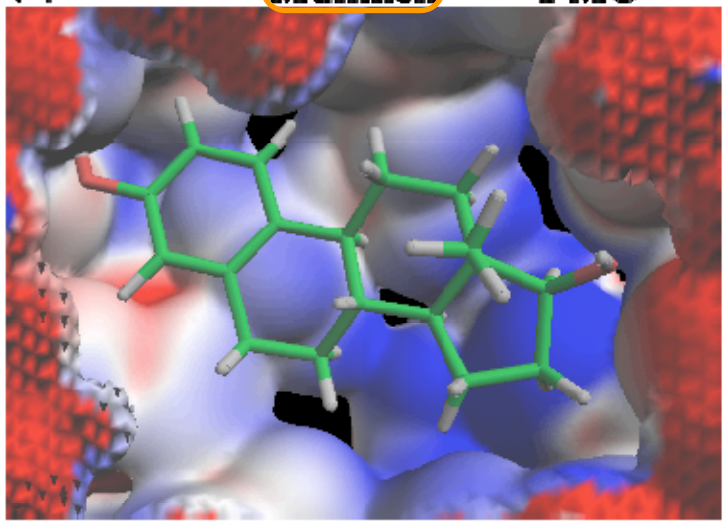

(b) $\Delta V = V_{\text{AMBER 94}} - V_{\text{FMO}}$

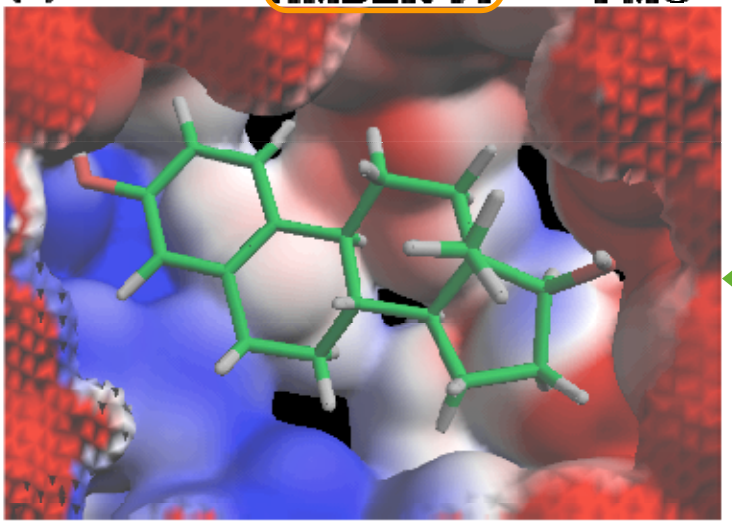

Deep:
Large diff.

(c) $\Delta V = V_{\text{Merz-Kollman}} - V_{\text{FMO}}$

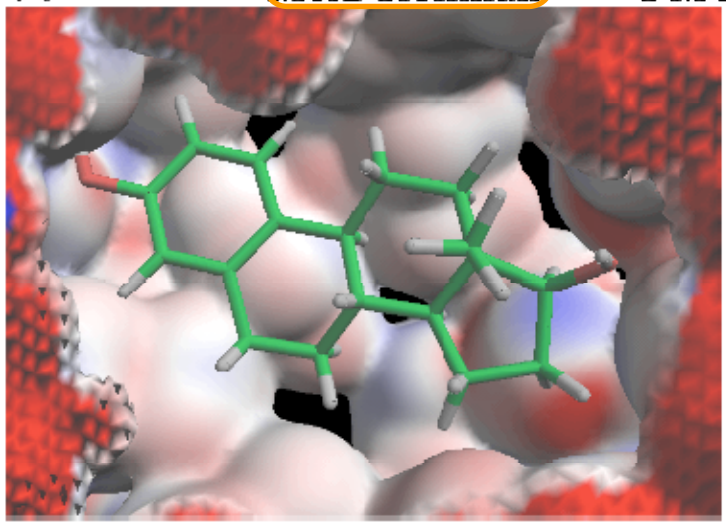

(d) $\Delta V = V_{\text{RESP}} - V_{\text{FMO}}$

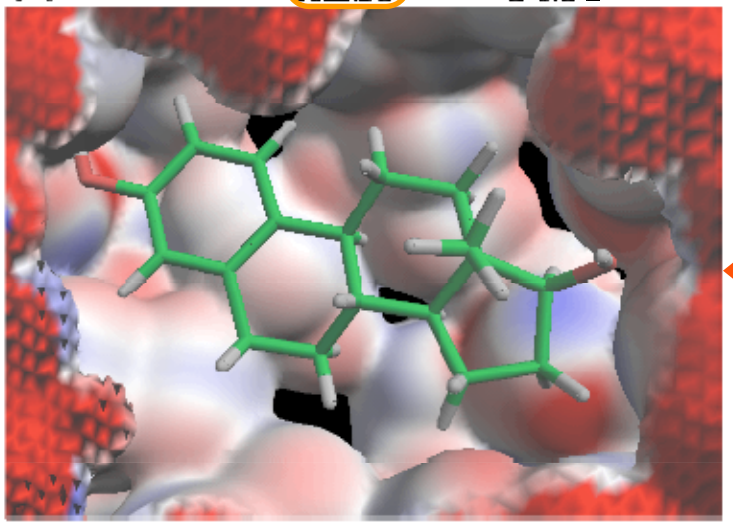

Light:
Small diff.

(a.u.)

(Y. Okiyama *et al*., Chem. Phys. Lett. 449 (2007) 329.)

MK vs. AMBER Charges in Crambin

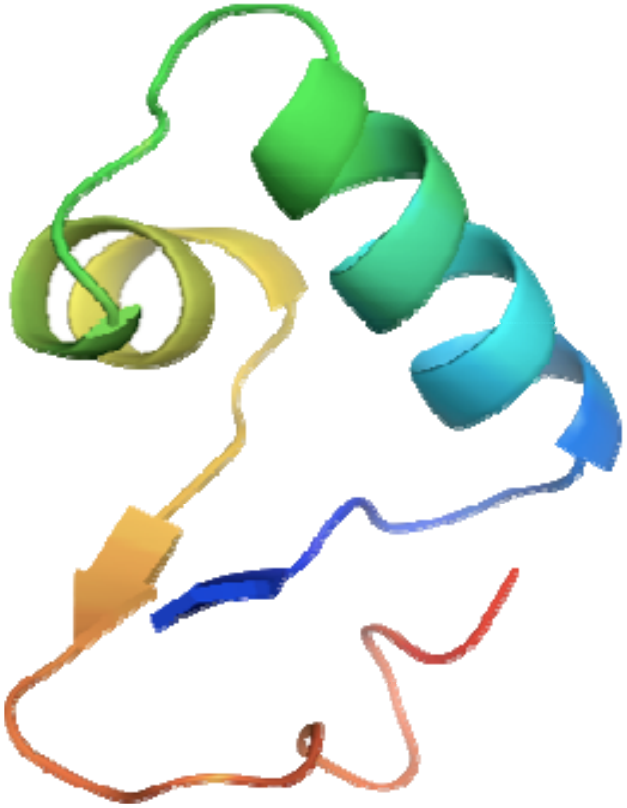

crambin (PDB ID: 1CCM)

46 residues (642 atoms)

Accuracy of ES potential

Charge	Deviation from QM
Merz-Kollman	1.9%
AMBER 94	27.5%

MK vs. AMBER charges

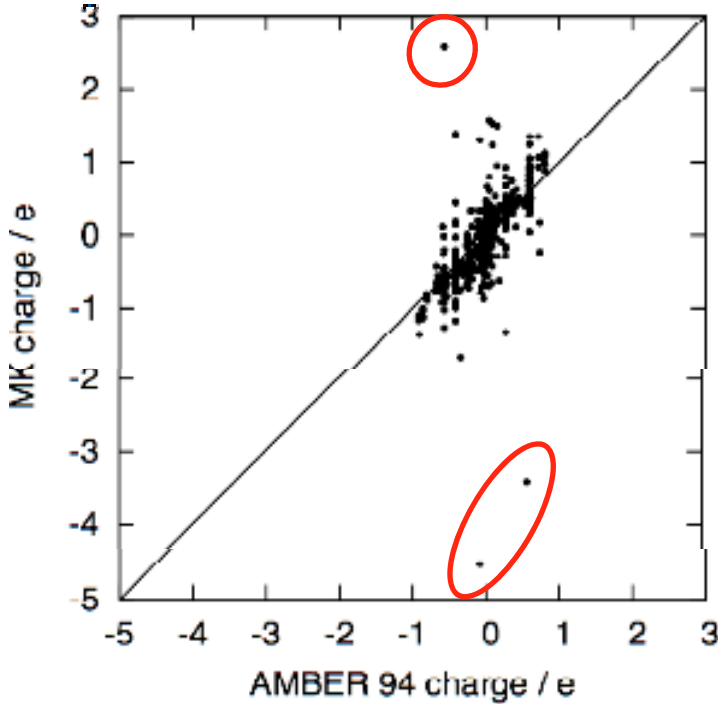

Restrained Fitting

W. Cornell et al., J. Am. Chem. Soc. 115 (1993) 9620.

Add a cost function due to the deviation from reference charges

$$\chi^2_{ESP'} = \chi^2_{ESP} + \chi^2_{harmonic}$$

Minimization

$$\chi^2_{harmonic} = k \sum_j (q_j - q_{0j})^2$$

Force constant (weight)

Reference charge

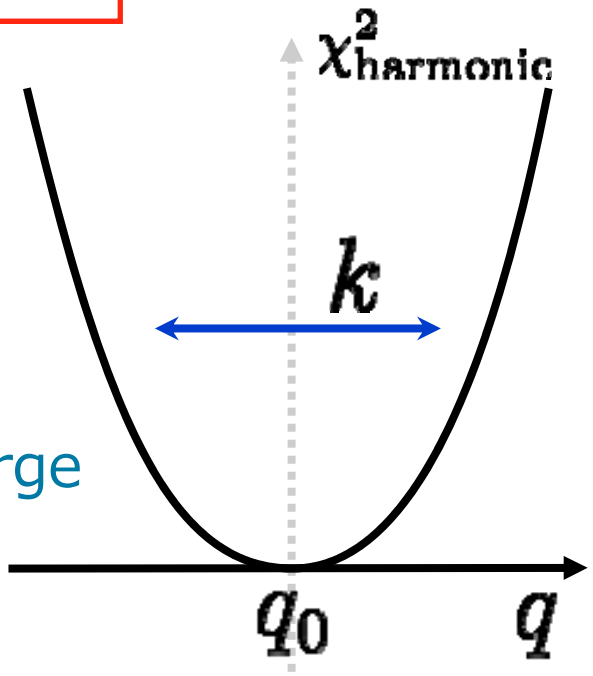

Reference charge: AMBER 94

- AMBER: well established force field
- Use of ESP charge (RESP)

Reproducibility of ES & Similarity of Charge

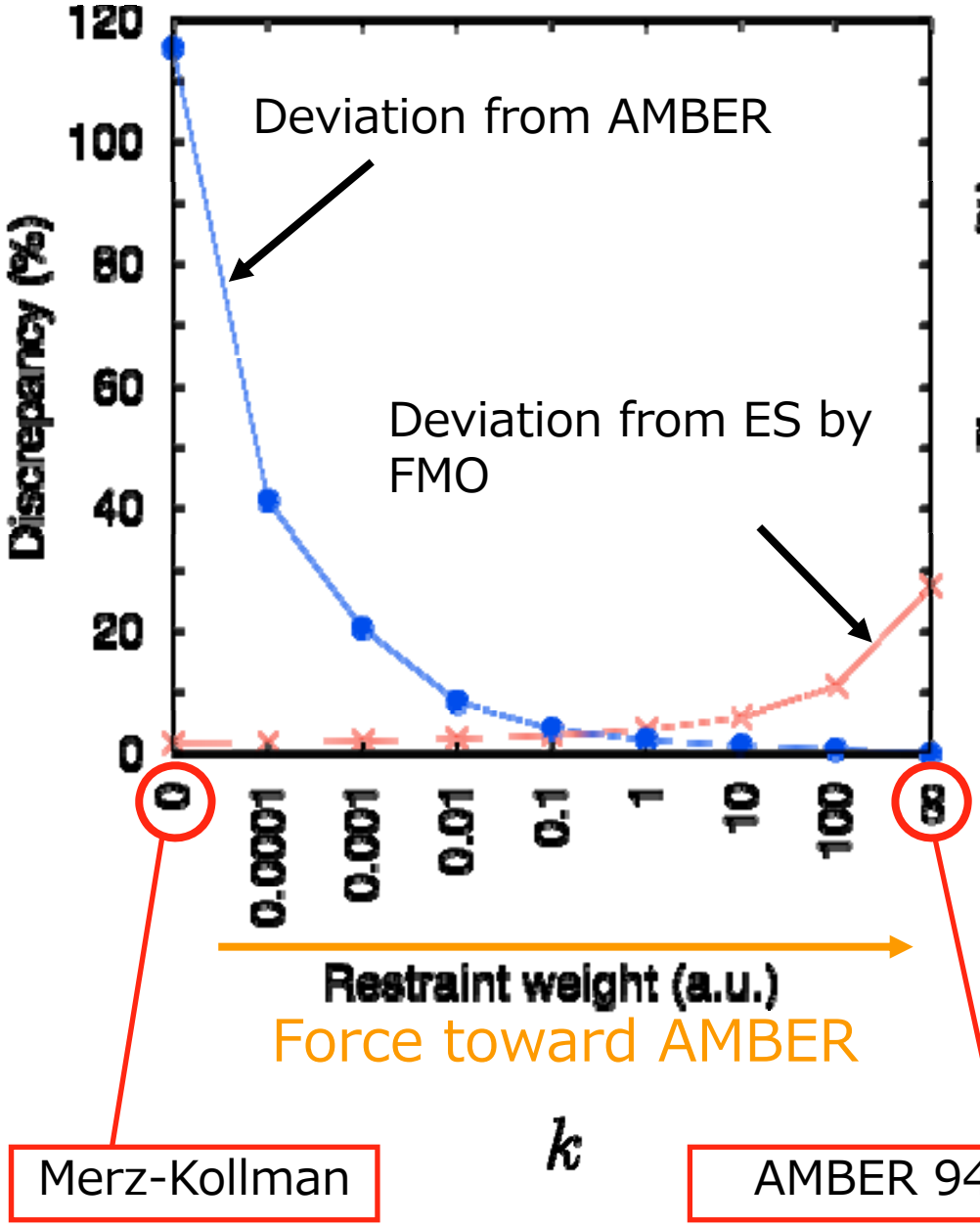

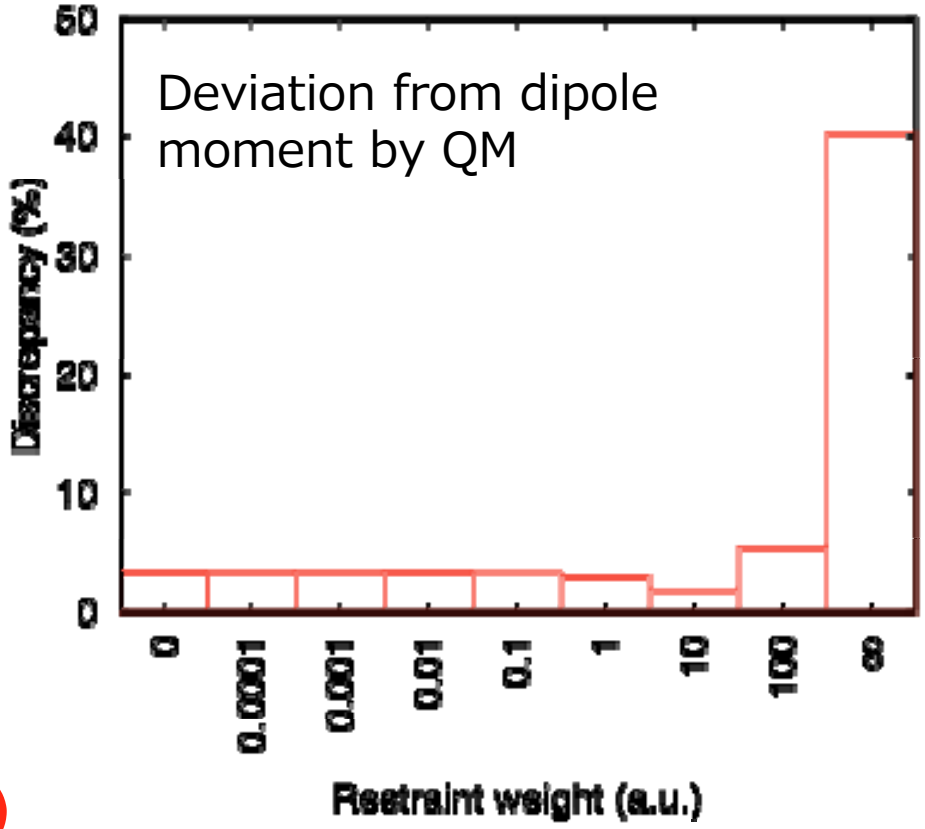

Approaching AMBER charges without loss of accuracy in ES

ESP vs. AMBER charges

Force toward AMBER charge

k=0 k=0.0001 k=0.001

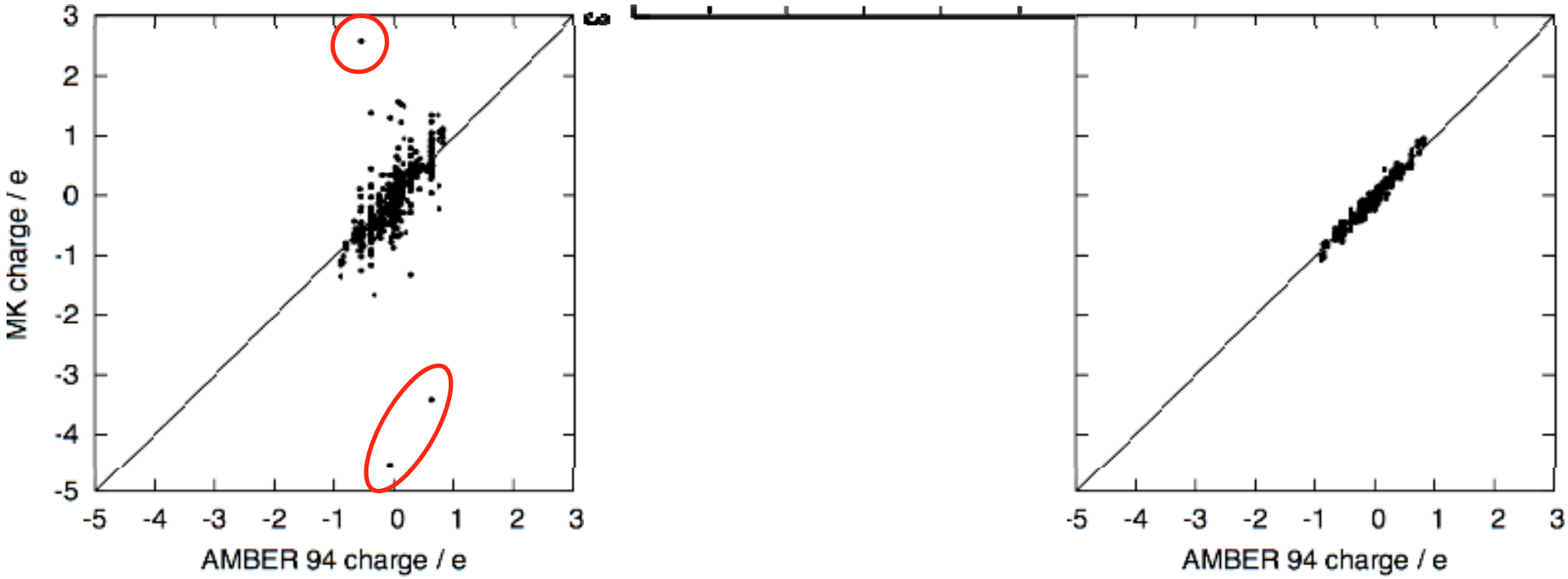

(Y. Okiyama et al., Chem. Phys. Lett. 467 (2009) 417.)

Ab Initio FMO-MD

◇*Ab initio* molecular dynamics

Forces by FMO @ ABINIT-MP ⇔ Trajectory @ PEACH

⇒ FMO2-HF （MP2 and FMO3 in progress）

Comparison with Car-Parrinello MD？

◇Application to hydrated formaldehyde

Blue shift in excitation energy

⇒ Benchmark system

Droplet model with 128 waters

FMO-HF/6-31G

⇒ 1 step/1.5 min. @ 20cores

⇒ several thousands step MD

Hundreds of sampling

⇒ MLFMO-CIS(D)/6-31G*

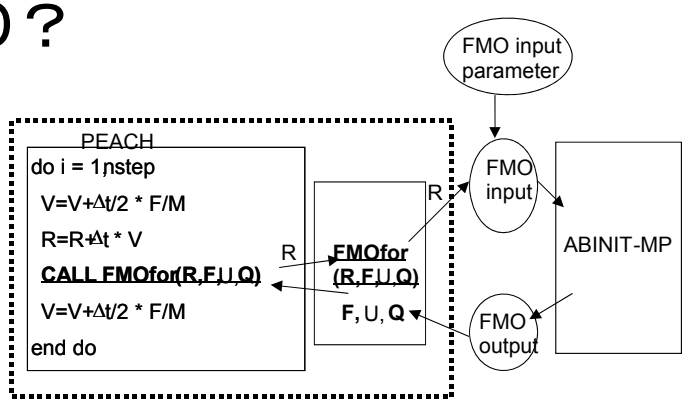

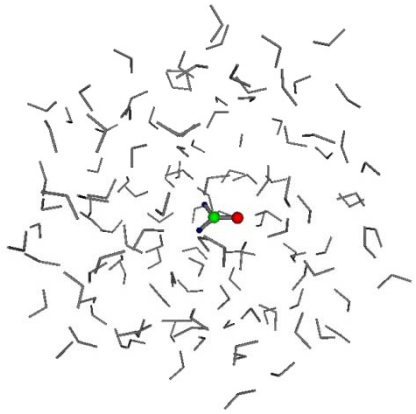

Good agreement with experiment

Ab Initio FMO-MD

400 samples

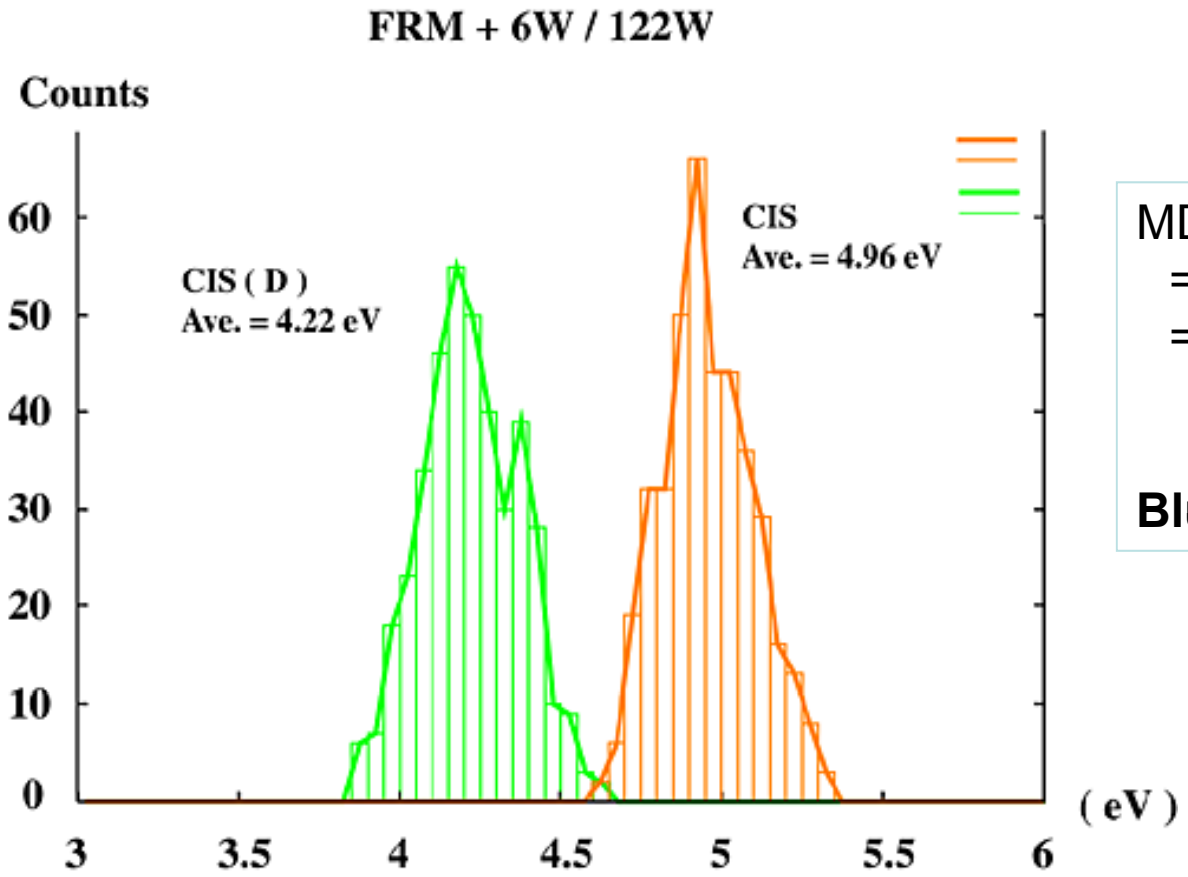

MD for gas-phase FRM
⇒ 4.56eV @ CIS
⇒ 4.08eV @ CIS(D)
(Expt.: 4.07eV)

Blue shift: +0.14eV @ CIS(D)

(Y. Mochizuki *et al*., Chem. Phys. Lett. 437 (2007) 66.)

Periodic Boundary Condition for FMO

$$E^{cell} = \sum_{I_0} E'_{I_0} + \frac{1}{2} \sum_{\mathbf{n}} \sum_{I_0 J_\mathbf{n}}{}' \Delta\widetilde{E}_{I_0 J_\mathbf{n}} + \sum_{\mathbf{n},\mathbf{n}'} \sum_{I_0 J_\mathbf{n} K_{\mathbf{n}'}}{}'' \Delta\widetilde{E}_{I_0 J_\mathbf{n} K_{\mathbf{n}'}}$$

$$\Delta\widetilde{E}_{I_0 J_\mathbf{n}} = E'_{I_0 J_\mathbf{n}} - E'_{I_0} - E'_{J_\mathbf{n}} + \mathrm{Tr}\left(\Delta\mathbf{D}^{I_0 J_\mathbf{n}} \mathbf{V}^{I_0 J_\mathbf{n}}\right)$$

$$\Delta\widetilde{E}_{I_0 J_\mathbf{n} K_{\mathbf{n}'}} = E'_{I_0 J_\mathbf{n} K_{\mathbf{n}'}} - E'_{I_0} - E'_{J_\mathbf{n}} - E'_{K_{\mathbf{n}'}} + \mathrm{Tr}\left(\Delta\mathbf{D}^{I_0 J_\mathbf{n} K_{\mathbf{n}'}} \mathbf{V}^{I_0 J_\mathbf{n} K_{\mathbf{n}'}}\right) - \Delta\widetilde{E}_{I_0 J_\mathbf{n}} - \Delta\widetilde{E}_{I_0 K_{\mathbf{n}'}} - \Delta\widetilde{E}_{J_\mathbf{n} K_{\mathbf{n}'}}$$

$$\mathbf{n} = (n_x, n_y, n_z)$$

$$n_x, n_y, n_z = 0, \pm 1, \pm 2, \ldots$$

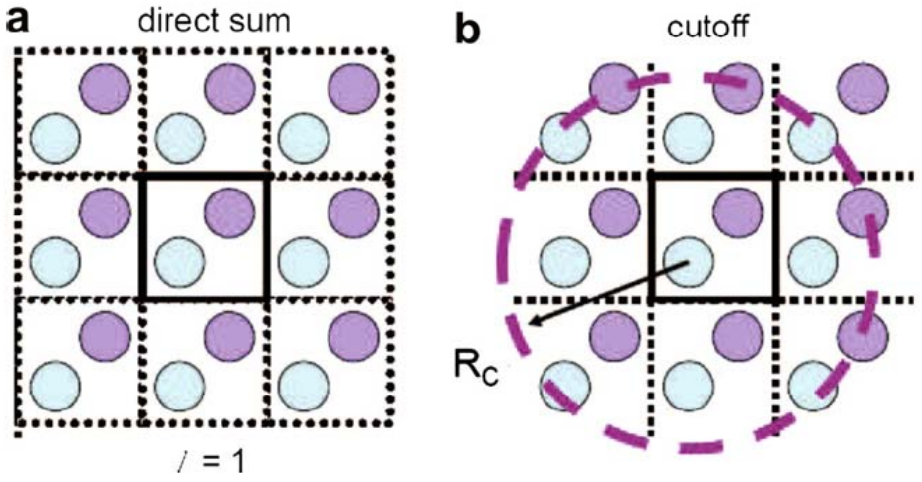

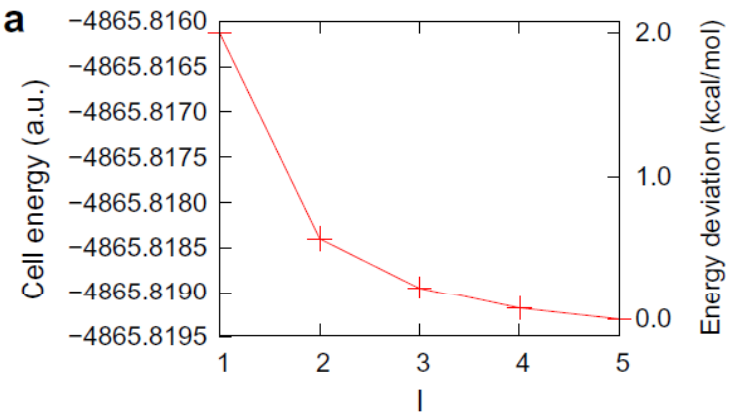

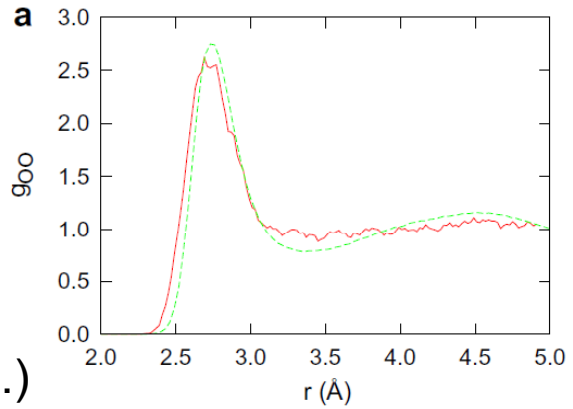

(T. Fujita *et al.*, Chem. Phys. Lett. 506 (2011) 112.)

Path Integral Molecular Dynamics Based on FMO

Electronic: FMO

$$E = \sum_{I_f}^{N_f} E_{I_f} + \sum_{I_f > J_f}^{N_f} \left(E_{IJ_f} - E_{I_f} - E_{J_f} \right)$$

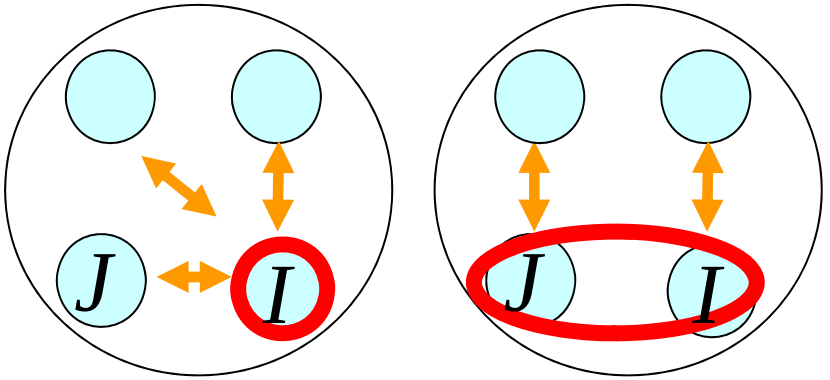

Monomer SCC　　Dimer SCF

Nuclear (Quantum & Temp.): PIMD

$$Z = \prod_{I=1}^{N} \left[\left(\frac{M_I P}{2\pi\beta\hbar^2} \right)^{\frac{3P}{2}} \int d\mathbf{R}_I^{(1)} \cdots d\mathbf{R}_I^{(P)} \right] \exp\left(-\beta V_{eff} \right)$$

$$V_{eff} = \sum_{s=1}^{P} \left[\sum_{I=1}^{N} \frac{M_I P}{2\beta^2\hbar^2} (\mathbf{R}_I^{(s)} - \mathbf{R}_I^{(s+1)})^2 + \frac{1}{P} E(\{\mathbf{R}^{(s)}\}) \right]_{\mathbf{R}^{(P+1)} = \mathbf{R}^{(1)}}$$

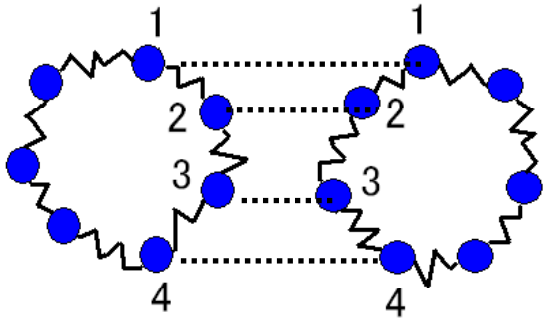

Quantum – Classical Isomorphism

(T. Fujita *et al.*, J. Phys. Soc. Jpn. 78 (2009) 104723.)

FMO-PIMD calculation for H_2O trimer（HF/6-31G**）

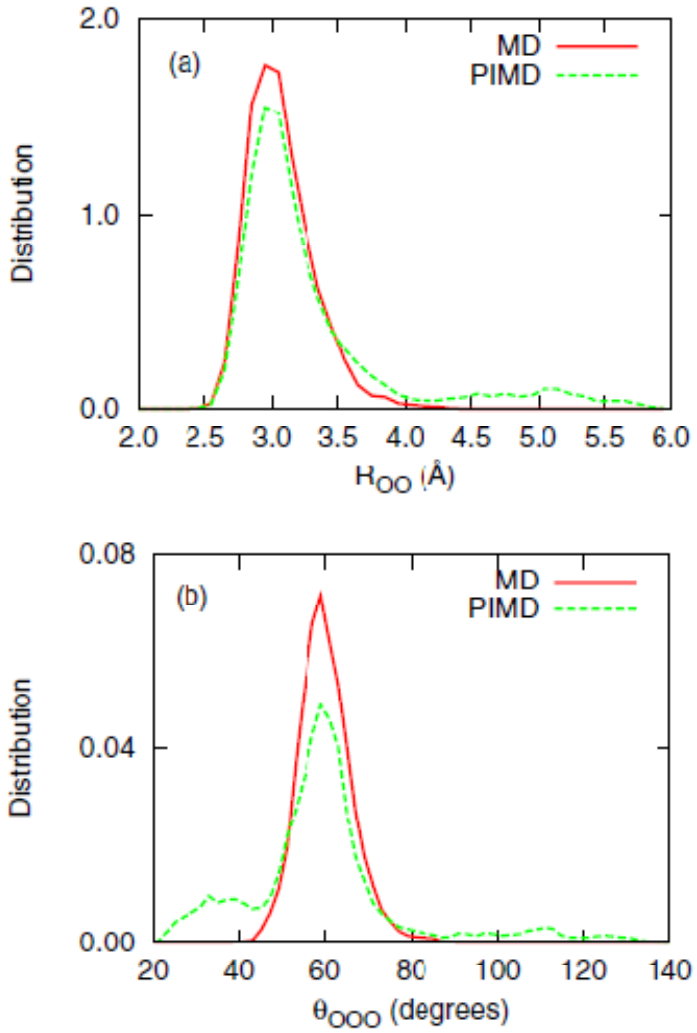

Fig. 2. (Color online) The probability distribution of (a) the O–O distances (R_{OO}) and (b) the O–O–O angles in the water trimer calculated by the MD (red and solid line) and the PIMD (green and dashed line) simulations. The results are shown in units of Å and deg.

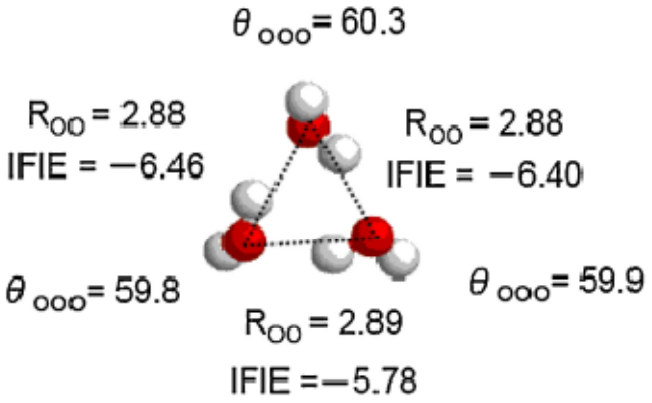

Fig. 1. (Color online) Optimized structure of water trimer calculated by FMO-HF/6-31G** method. The O–O distances (R_{OO}), the O–O–O angles (θ_{OOO}), and the interfragment interaction energies (IFIEs) are shown in unit of Å, deg, and kcal/mol, respectively. Red and white balls refer to the oxygen and hydrogen atoms, respectively.

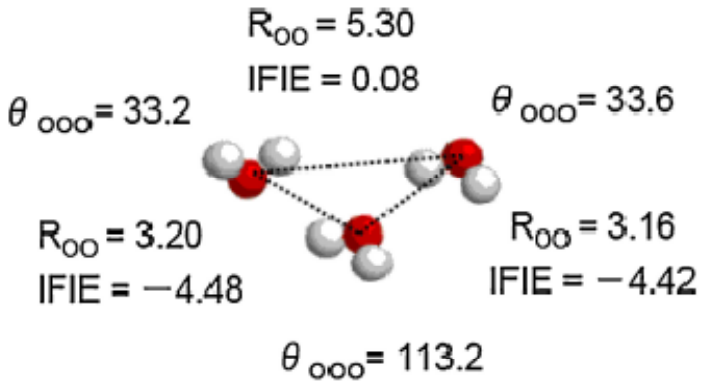

Fig. 3. (Color online) One of snapshots in the PIMD simulation for water trimer. The picture only shows the centroid coordinates, $\sum_{s=1}^{P} R_I^{(s)}/P$. The O–O distances ($R_{OO}$), the O–O–O angles ($\theta_{OOO}$), and the interfragment interaction energies (IFIEs) are shown in units of Å, deg, and kcal/mol, respectively.

Electron Transfer Rate in Biomolecular Systems

$$k_{\mathrm{DA}} = \frac{2\pi}{\hbar}\langle \sum_{\mathrm{v}} |\langle \Psi_{\mathrm{iu}}(\vec{r},\vec{R})|\hat{T}^{\mathrm{DA}}|\Psi_{\mathrm{fv}}(\vec{r},\vec{R})\rangle_{\vec{r},\vec{R}}|^2 \delta(E_{\mathrm{iu}} - E_{\mathrm{fv}})\rangle_{\mathrm{T}},$$

$$k_{\mathrm{DA}} = \frac{1}{\hbar^2}\int_{-\infty}^{\infty} dt\ \langle T^{\mathrm{qc}}_{\mathrm{DA}}(t) T^{\mathrm{qc}}_{\mathrm{AD}}(0)\rangle_{\mathrm{T}} \langle I(t)\rangle_{\mathrm{T}}.$$

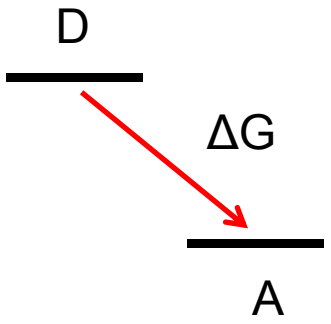

$$\langle I(t)\rangle_{\mathrm{T}} = \exp\left[-\frac{i}{\hbar}(\Delta G + \lambda)\, t - \frac{1}{\hbar^2}\int_0^t d\tau \int_0^\tau d\tau' C(\tau')\right],$$

$$C(t) = \frac{2\hbar}{\pi}\int_0^\infty d\omega\ J(\omega)\left[\coth\left(\frac{\hbar\omega}{2k_{\mathrm{B}}T}\right)\cos\omega t - i\sin\omega t\right]$$

Spectral density

Electronic tunneling

$$k_{\mathrm{DA}} = \frac{2\pi}{\hbar^2}\int_{-\infty}^{\infty} d\varepsilon \frac{2}{1+\exp(-\varepsilon/k_{\mathrm{B}}T)} \frac{1}{2\pi\hbar}\int_{-\infty}^{\infty} dt\ \langle T_{\mathrm{DA}}(t) T_{\mathrm{DA}}(0)\rangle_{\mathrm{T}} \exp\left(\frac{i\varepsilon t}{\hbar}\right)$$
$$\times \frac{1}{2\pi}\int_{-\infty}^{\infty} d\tau \exp\left[-Q_2(\tau) - iQ_1(\tau)\right] \exp\left[-i\frac{(\Delta G + \varepsilon)}{\hbar}\tau\right],$$

Bath coupling

ET rate can be estimated in terms of temporal correlation functions obtained through MD and FMO.

(ST and E.B. Starikov, Phys. Rev. B 81 (2010) 027101.)

$$Q_1(t) = \frac{2}{\pi\hbar}\int_0^\infty \frac{d\omega}{\omega^2} J(\omega)\sin\,\omega t \qquad Q_2(t) = \frac{2}{\pi\hbar}\int_0^\infty \frac{d\omega}{\omega^2} J(\omega)\coth\left(\frac{\hbar\omega}{2k_BT}\right)(1-\cos\,\omega t).$$

$$\lambda = \frac{2}{\pi}\int_0^\infty \frac{d\omega}{\omega} J(\omega),$$

$$A(t) = [\langle T_{DA}(t)T_{DA}(0)\rangle_T - \langle T_{DA}\rangle_T^2]/(\langle T_{DA}^2\rangle_T - \langle T_{DA}\rangle_T^2),$$

$$A(t) = \exp[-\gamma|t|] \qquad \gamma = 1/\tau_c.$$

(inelastic electron tunneling and nuclear quantum effects)

Test calculations using the dielectric function of water

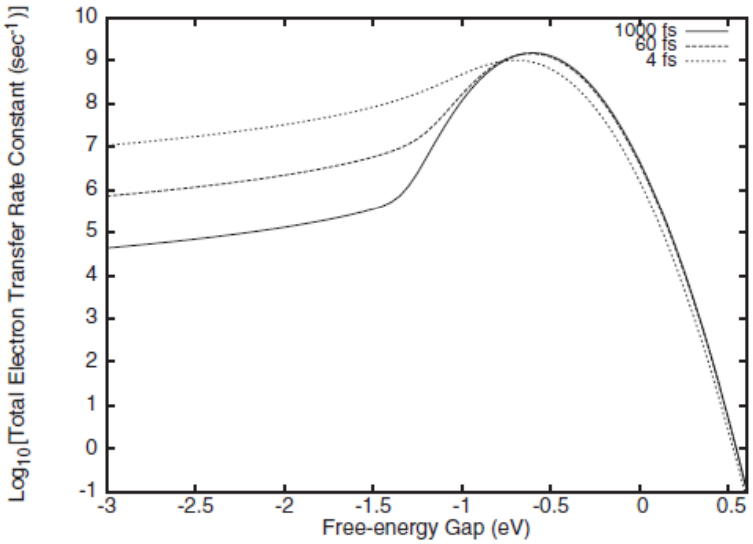

FIG. 1. ET rate constant $k_{DA}(\Delta G)$ calculated by Eq. (18) in the case of $\lambda = 0.6$ eV for $\tau_c = 4$ fs (dotted line), 60 fs (dashed line), and 1000 fs (solid line).

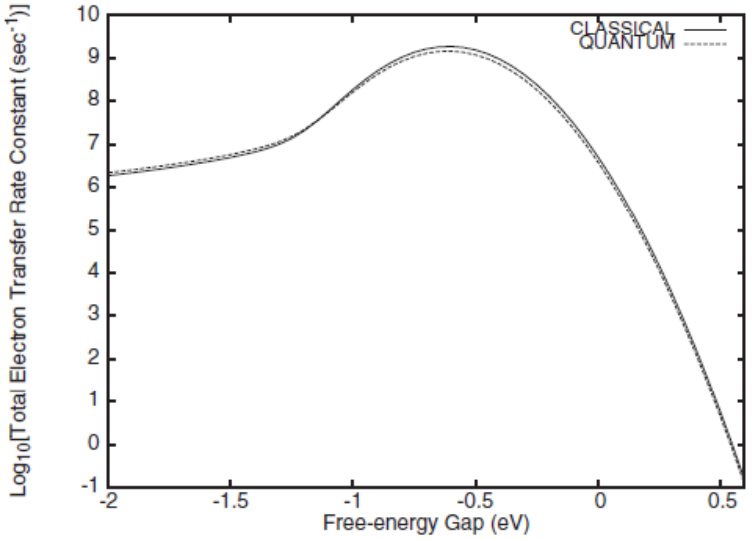

FIG. 2. Comparison of ET rate constants calculated by Eq. (18) (dashed line) and Eq. (23) (solid line) in the case of $\tau_c = 60$ fs and $\lambda = 0.6$ eV.

Excitation Energy Transfer in FMO Protein

Fenna-Matthews-Olson (FMO) light-harvesting protein connects the outer antenna system (chlorosome/baseplate) with the reaction center in green sulfur bacteria.

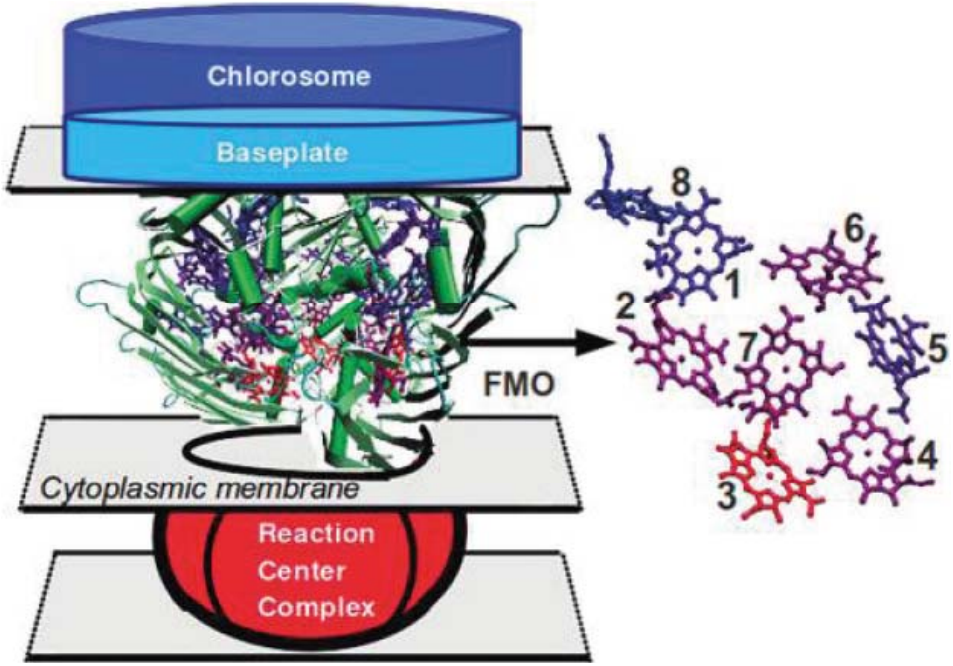

(Schmidt *et al.*, 2011)

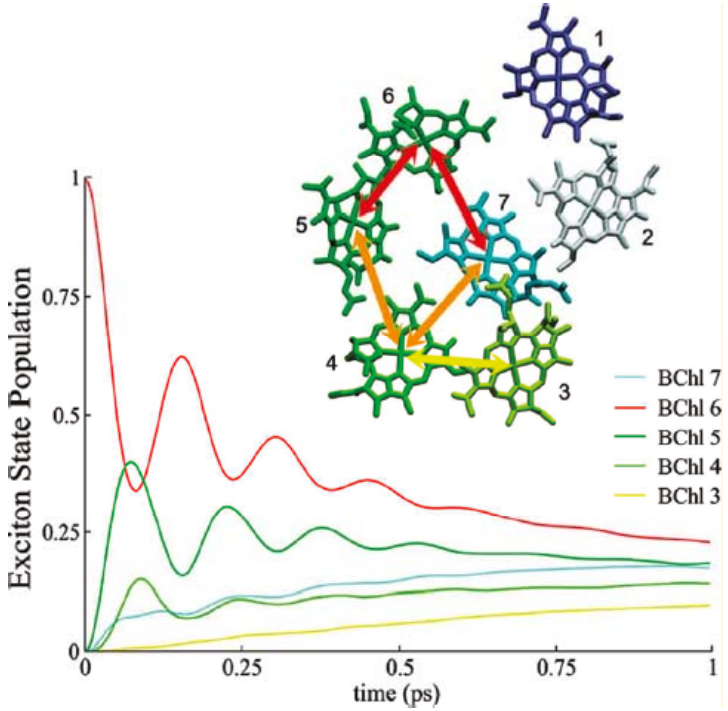

(Kelly *et al.*, 2011)

The FMO complex has recently become a paradigmatic model system in terms of the long-lived electronic quantum coherence associated with highly efficient excitation energy transfer that has been experimentally observed in photosynthetic systems.

Ab initio description for excitation energy transfer (I)

$$H = H_0 + V_0,$$ Homodimer embedded in biomolecular environment

$$H_0 = H_D|D\rangle\langle D| + H_A|A\rangle\langle A|$$

$$V_0 = J\left(|A\rangle\langle D| + |D\rangle\langle A|\right)$$

$$i\hbar\frac{\mathrm{d}\rho_I(t)}{\mathrm{d}t} = [V_I(t), \rho_I(t)] \equiv L_I(t)\rho_I(t)$$ Liouville-von Neumann equation

$$i\hbar\frac{\mathrm{d}}{\mathrm{d}t}\left[\mathcal{P}\rho_I(t)\right]$$

P, Q=1-P : Projection operators

$$= \mathcal{P}L_I(t)\mathcal{P}\rho_I(t)$$

$$+\mathcal{P}L_I(t)\exp_+\left[-\frac{i}{\hbar}\int_0^t \mathrm{d}t_1 \mathcal{Q}L_I(t_1)\right]\mathcal{Q}\rho_I(0)$$

$$-\frac{i}{\hbar}\int_0^t \mathrm{d}t_1 \mathcal{P}L_I(t)\exp_+\left[-\frac{i}{\hbar}\int_{t_1}^t \mathrm{d}t_2 \mathcal{Q}L_I(t_2)\right]\mathcal{Q}L_I(t_1)\mathcal{P}\rho_I(t_1)$$

Ab initio description for excitation energy transfer (II)

$$\frac{\mathrm{d}}{\mathrm{d}t}P_D(t) = \int_0^t \mathrm{d}t_1 \left[-M\left(t,t_1\right) P_D\left(t_1\right) + M\left(t,t_1\right) P_A\left(t_1\right)\right]$$

$$\frac{\mathrm{d}}{\mathrm{d}t}P_A(t) = \int_0^t \mathrm{d}t_1 \left[M\left(t,t_1\right) P_D\left(t_1\right) - M\left(t,t_1\right) P_A\left(t_1\right)\right]$$

$$\begin{aligned} M(t,t_1) &= \frac{1}{\hbar^2}\langle V_{DA}(t)V_{AD}(t_1) + V_{DA}(t_1)V_{AD}(t)\rangle \\ &= \frac{1}{\hbar^2}\langle V_{AD}(t)V_{DA}(t_1) + V_{AD}(t_1)V_{DA}(t)\rangle \end{aligned}$$

$$M(t,t_1) = \frac{2J_0^2}{\hbar^2}\exp\left(-\frac{t-t_1}{\tau_0}\right)\cos\left[\omega_0\left(t-t_1\right)\right]$$

<u>Model calculation</u>

τ_0 = 100 fs, ω_0^{-1} = 100 fs
$\hbar/J_0$ = 1000, 400, 100, 10 fs

(ST, Chem. Phys. Lett. 508 (2011) 139.)

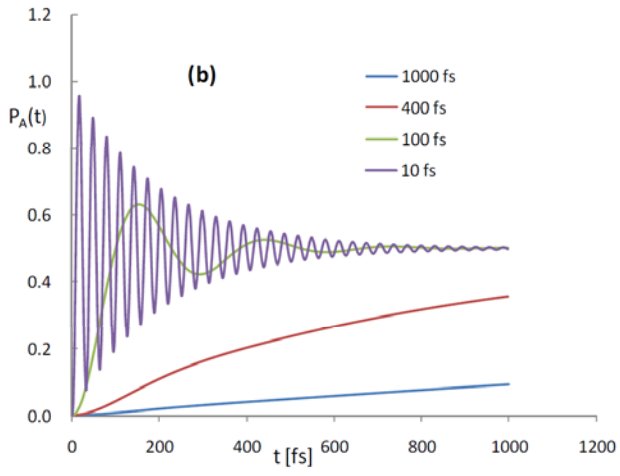

Ab Initio Descriptions of Reaction Dynamics

- Electron and energy transfer in biomolecular systems can be described in ab initio way in terms of (temporal) correlation functions obtained through molecular dynamics and molecular orbital calculations.
- Fast (FMO) calculations of electronic states for many conformations would be essential for accurate evaluations of population dynamics and rate constant.

Collaborators

- Yuji Mochizuki (Rikkyo Univ.)
- Kaori Fukuzawa (Mizuho IRI)
- Tatsuya Nakano (NIHS)
- Katsumi Yamashita (NEC Soft)
- Jewgeni Starikov (RC Karlsruhe)
- Yoshio Okiyama (Tokyo Univ.)
- Hirofumi Watanabe (RIKEN)
- Takatoshi Fujita (Kobe Univ.)